Original Article

MOLECULAR METABOLISM

Maternal obesity persistently alters cardiac progenitor gene expression and programs adult-onset heart disease susceptibility

Abdalla Ahmed [1,2], Minggao Liang [2,3], Lijun Chi [1], Yu-Qing Zhou [4], John G. Sled [4,5], Michael D. Wilson [2,3], Paul Delgado-Olguín [1,2,6,*]

ABSTRACT

Objective: Heart disease risk can be programmed by intrauterine exposure to obesity. Dysregulating key transcription factors in cardiac progenitors can cause subsequent adult-onset heart disease. In this study, we investigated the transcriptional pathways that are altered in the embryonic heart and linked to heart disease risk in offspring exposed to obesity during pregnancy.

Methods: Female mice were fed an obesogenic diet and mated with males fed a control diet. Heart function and genome-wide gene expression were analyzed in adult offspring born to obese and lean mice at baseline and in response to stress. Cross-referencing with genes dysregulated genome-wide in cardiac progenitors from embryos of obese mice and human fetal hearts revealed the transcriptional events associated with adult-onset heart disease susceptibility.

Results: We found that adult mice born to obese mothers develop mild heart dysfunction consistent with early stages of disease. Accordingly, hearts of these mice dysregulated genes controlling extracellular matrix remodeling, metabolism, and TGF-β signaling, known to control heart disease progression. These pathways were already dysregulated in cardiac progenitors in embryos of obese mice. Moreover, in response to cardiovascular stress, the heart of adults born to obese dams developed exacerbated myocardial remodeling and excessively activated regulators of cell-extracellular matrix interactions but failed to activate metabolic regulators. Expression of developmentally regulated genes was altered in cardiac progenitors of embryos of obese mice and human hearts of fetuses of obese donors. Accordingly, the levels of *Nkx2-5*, a key regulator of heart development, inversely correlated with maternal body weight in mice. Furthermore, Nkx2-5 target genes were dysregulated in cardiac progenitors and persistently in adult hearts born to obese mice and human hearts from pregnancies affected by obesity.

Conclusions: Obesity during pregnancy alters Nkx2-5-controlled transcription in differentiating cardiac progenitors and persistently in the adult heart, making the adult heart vulnerable to dysregulated stress responses.

© 2020 The Authors. Published by Elsevier GmbH. This is an open access article under the CC BY-NC-ND license (http://creativecommons.org/licenses/by-nc-nd/4.0/).

Keywords Heart disease susceptibility; Fetal programming of heart disease; Maternal obesity; Cardiac progenitors; Gene expression; Nkx2-5; Myocardial remodeling

1. INTRODUCTION

Maintenance of a homeostatic *in utero* environment during pregnancy is required for proper embryonic development and long-term health of offspring. Several epidemiological studies and animal models have shown that the risk of adult-onset disease can be determined during embryonic development. This is known as "fetal programming."

Obesity during pregnancy poses a significant deviation from *in utero* homeostasis by promoting inflammation, perturbing placental and fetal perfusion, and causing metabolic imbalance [1]. *In utero* exposure to obesity has long-lasting deleterious effects in offspring such as increased long-term risk of hospitalization and mortality due to cardiovascular disease [2—4]. This risk is proportional to the absolute maternal body mass index (BMI); as maternal BMI increases, there is a continuous increase in risk for offspring [2—4]. Abnormal gestational weight gain is also associated with increased mortality or heart transplants in children with congenital heart disease [5], indicating that the fetal environment can alter disease risk trajectory in offspring. Obesity during pregnancy is also associated with heart dysfunction during the first trimester and persistently throughout gestation [6,7]. Fetal cardiac dysfunction manifests as alterations in cardiac blood flow dynamics followed by changes in ventricular chamber dimensions [6,7]. Obesity during pregnancy also leads to cardiac defects in offspring in animal models including sheep, fly, and mice [1,8—12]. For example, in *Drosophila*, a maternal high-fat diet leads to cardiac lipotoxicity and contractile dysfunction in adult offspring [12]. Adult

[1]Translational Medicine, Hospital for Sick Children, Toronto, Ontario, M5G 0A4, Canada [2]Department of Molecular Genetics, University of Toronto, Toronto, Ontario, M5S 1A8, Canada [3]Genetics & Genome Biology, Hospital for Sick Children, Toronto, Ontario, M5G 0A4, Canada [4]Mouse Imaging Center, Hospital for Sick Children, Toronto, Ontario, M5T 3H7, Canada [5]Department of Medical Biophysics, University of Toronto, Toronto, Ontario, M5G 1L7, Canada [6]Heart & Stroke Richard Lewar Center of Excellence, Toronto, Ontario, M5S 3H2, Canada

*Corresponding author. Translational Medicine, Hospital for Sick Children, Toronto, Ontario, M5G 0A4, Canada. E-mail: paul.delgadoolguin@sickkids.ca (P. Delgado-Olguín).

Received September 10, 2020 • Revision received November 8, 2020 • Accepted November 12, 2020 • Available online 17 November 2020

https://doi.org/10.1016/j.molmet.2020.101116

 © 2020 The Authors. Published by Elsevier GmbH. This is an open access article under the CC BY-NC-ND license (http://creativecommons.org/licenses/by-nc-nd/4.0/).

mice born to obese dams develop transient cardiac hypertrophy and reduced systolic function [9,13]. However, how obesity during pregnancy translates into an increased risk of heart disease in offspring remains unclear.

Heart development is a tightly regulated multistep process particularly vulnerable to alterations of the *in utero* environment during early stages of cardiogenesis. For example, hyperglycemia impairs heart tube formation in the chick embryo [14] and left—right axis establishment in the mouse heart [15]. Key transcription factors establish programs that drive differentiation of cardiac progenitors (CPs), coordinate heart development, and maintain long-term gene expression. The transcription factor Nk2 homeobox 5 (Nkx2-5) is at the core of cardiac gene regulatory networks and required for long-term stability of the cardiac gene expression program [16]. Nkx2-5 is first expressed during early development in CPs and continuously in the adult heart [17]. Nkx2-5 regulates important processes that are altered in heart disease such as fibrosis, energy metabolism, conduction, and cardiomyocyte contraction. Nkx2-5 is a key repressor of myofibroblast differentiation, which contributes to extracellular matrix (ECM) deposition in the heart [18]. Nkx2-5 is also responsive to and regulates cardiac metabolism. Nkx2-5 levels are decreased in the hearts of diabetic mice [19], and point mutations affecting its activity lead to decreased mitochondrial respiration and heart function [20]. *Nkx2-5* and downstream targets are also dysregulated in a zebrafish model of hyperglycemia [21]. Perinatal Nkx2-5 loss of function leads to conduction defects through reduced expression of several ion channels, including *Scn5a* and *Ryr2* [22]. Dominant negative mutations in *Nkx2-5* also lead to fibrosis and a reduced contractile function, which are exacerbated upon injury with doxorubicin, indicating a protective function of Nkx2-5 against stress [23]. Deregulation of pathways controlled by Nkx2-5 in differentiating mouse CPs can have negative long-term effects on the postnatal heart. For example, persistent overexpression of homeodomain transcription factor *Six1*, an Nkx2-5 target, in CPs causes hypertrophic cardiomyopathy in adulthood [24]. However, the long-term effects of obesity during pregnancy in gene expression in CPs and the adult heart and the transcriptional pathways that program a higher risk of heart disease in offspring are unknown.

In this study, we investigated the long-term effects of maternal obesity in gene expression in CPs, adult mouse hearts, and human fetal hearts exposed to obesity *in utero*.

2. METHODS

2.1. Mice

All animal procedures were approved by the Animal Care Committee at the Center for Phenogenomics and were in compliance with the NIH Guide for the Care and Use of Laboratory Animals. All experiments were conducted on Nkx2-5tg mice [25]. Female mice were fed irradiated diets ad libitum: control diet (10% fat and 1% sucrose kcal; D12450K) or high-fat/high-sugar diets (33% fat and 30% sucrose by kcal; D13052905) obtained from Research Diets, Inc., beginning at 4 weeks of age and throughout their lifetime. The female mice were first mated with male mice at 12 weeks of age and only their second litters were used for the experiments. All male mice used for breeding were fed control diets except during breeding. All male offspring were weaned onto control diets at P21. The mice were housed in standard vented cages in temperature- and humidity-controlled rooms with 12-h light—dark cycles (21—22 °C and 30—60% humidity), and free access to water and food. For mouse embryo studies, the presence of vaginal plugs indicated E0.5. Somites were counted to determine the embryonic stage, with 21—25 somites indicating E9.5.

2.2. Human fetal heart samples

The samples were collected through the Research Center for Women and Infant Health (RCWIH) BioBank (Mount Sinai Health System, Toronto, Ontario, Canada). The studies were approved by the Ethics Research Boards at the Hospital for Sick Children and Mount Sinai Hospital. The fetal hearts were obtained from healthy donors undergoing elective pregnancy termination. Terminations due to congenital defects were excluded. The fetal hearts were dissected by a qualified nurse and frozen in RNAlater Stabilization Solution (Thermo Fisher Scientific) solution at −80 °C.

2.3. Adverse myocardial remodeling induction

Osmotic pumps (ALZET) were filled with isoproterenol (60 mg/kg/day in PBS) and implanted subdermally in 8-week-old mice for 14 days. The mice were anesthetized using isoflurane (1.5%) for implantation. The mice were administered Metacam (2 mg/kg) for analgesia once daily for three days via subcutaneous injections, with the first dose given preemptively before implantation.

2.4. Metabolic analysis

Body weight was measured weekly. Body composition was measured using a body composition analyzer (EchoMRI-100 machine, Echo Medical Systems, Houston, TX, USA) on unanesthetized mice. Glucose tolerance tests were conducted on the mice after 16 h of fasting with water ad libitum by intraperitoneal injections of glucose (1 mg/g of body weight). Blood glucose was measured at 0, 15, 30, 60, and 120 min post-injection using a glucometer (Contour NEXT, Bayer HealthCare).

2.5. Echocardiography

Cardiac morphology and function were evaluated in male offspring born to CD- or HD-fed dams using a high-frequency Vevo2100 ultrasound imaging system (VisualSonics, Toronto, Canada) with a 30 MHz transducer. All mice were scanned for 20—30 min under light isoflurane (1.5%) anesthesia. Each mouse's body temperature was carefully monitored using a rectal thermometer and maintained at ∼37 °C using a heated platform and a heat lamp. Left ventricular dimensions and systolic and diastolic functions were measured as previously described [26].

2.6. Blood pressure and heart rate measurements

A CODA Monitor Noninvasive Blood Pressure System (Kent Scientific Corporation) was used to measure the blood pressure and heart rate of the unanesthetized mice. The mice were placed in holders on warming platforms and their temperature was carefully monitored using an infrared thermometer. All mice were acclimated to the system for 2 days before data acquisition by placing them in the holders for 20 min on the warming platforms with the cuff on their tail. Recordings were collected on days 3, 4, and 5 after acclimation. A total of 20 recording cycles were conducted for each mouse on each day, and the last 10 recordings were averaged. The average readings of the three days were used for analysis. All acclimations and recordings were conducted between 3 and 5 pm to avoid variations known to be induced by circadian rhythms [27]. Appropriate holder and cuff sizes were selected according to the mouse weight according to the manufacturer's instructions.

 © 2020 The Authors. Published by Elsevier GmbH. This is an open access article under the CC BY-NC-ND license (http://creativecommons.org/licenses/by-nc-nd/4.0/).

2.7. Histology

Hearts dissected in cold PBS were prepared for paraffin embedding as previously described [28]. The hearts were sectioned into 7-μm-thick sections and stained by Masson's trichrome.

2.8. Immunofluorescence

The dissected hearts were fixed in 4% PFA overnight at 4 °C, washed in PBS three times for 10 min at room temperature, and maintained in 30% sucrose/PBS at 4 °C overnight or until the tissues sank. The hearts were embedded in OCT compound and sectioned to 7 μm thick. Cardiomyocyte size was measured using sections stained with wheat germ agglutinin (W11262 Invitrogen) [24]. Immunostaining was conducted as previously described [28]. Antibodies used were anti-COL5A1 (Santa Cruz Biotechnology, sc-20648, 1:200), anti-GFP (GeneScript, A01694, 1:1000), and anti-ISL1 (Developmental Studies Hybridoma Bank, 40.2D6, 1:100).

2.9. Cell sorting

eGFP-positive embryos were identified under a Nikon SMZ1500 microscope. Embryos with 20–25 somites were dissociated and the cells were sorted as previously described [29]. Embryos were pooled together before sorting for qPCR or sorted individually for RNA-seq.

2.10. RNA extraction

For adult hearts, whole ventricles were dissected and frozen in TRIzol immediately after dissection. The hearts were homogenized at 30 kHz for 1 min using TissueLyser II (Qiagen). The homogenized samples were centrifuged to pellet insoluble tissue. A Direct-zol RNA MiniPrep kit (Zymo Research) was used to isolate DNA-free RNA.

To isolate RNA from CPs, the sorted cells were lysed in TRIzol and RNA was extracted using phenol-chloroform.

To isolate RNA from human fetal tissue, whole hearts were stored in RNAlater Stabilization Solution (Thermo Fisher Scientific) and frozen immediately after isolation. The hearts were later thawed and the ventricles were dissected away from the atria and major vessels. The ventricles were cut open and rinsed for 10 s in PBS to remove blood inside the chamber and then immediately placed in TRIzol. The ventricles were homogenized at 30 kHz for 1 min using TissueLyser II (Qiagen). Homogenized samples were centrifuged to pellet insoluble tissue. A Direct-zol RNA MiniPrep kit (Zymo Research) was used to isolate DNA-free RNA.

2.11. Gene expression analysis

cDNA prepared using a SuperScript III First-Strand Synthesis Kit (Invitrogen) was used for qPCR analysis. Advanced qPCR Master Mix with Supergreen Dye Low ROX (Wisent) was used for qPCR analysis on a CFX384 Touch Real-Time PCR Detection System (Bio-Rad). All samples were run in triplicate. Data were analyzed using CFX Manager Software (Bio-Rad).

For 32-week-old adult hearts, RNA-seq libraries were prepared using a NEBNext Ultra RNA Library Prep Kit for Illumina with the NEBNext Poly(A) mRNA Magnetic Isolation Module and 1 ug of starting material. Single-end sequencing (50 bp) was performed on an Illumina HiSeq 2500 platform.

For 2-month-old mice treated with isoproterenol and human fetal hearts, a NEBNext Ultra II RNA Library Prep Kit for Illumina was used with the NEBNext Poly(A) mRNA Magnetic Isolation Module and 1 ug of starting material. Single-end sequencing (50 bp) was performed on an Illumina Hi-Seq 2500 platform.

For the CPs, Ovation SoLo RNA-Seq Systems (NuGEN) for mice was used with 9 ng of total RNA as a starting material.

2.12. RNA-seq analysis

Raw sequence reads were trimmed using Trimmomatic 0.36 [30] and aligned to the reference mouse genome (mm10) or human genome (hg38) using STAR version 2.5.3 [31]. Total counts were quantified using FeatureCounts [32] and normalized using DESeq2 version 1.22.21 (with batch correction) [33]. Adjusted P values < 0.05 were considered significant. For the CPs, reads were de-duplicated using NuDup (https://www.nugentechnologies.github.io/nudup/). All of the PCA plots were generated using Plotly [34] in R. Differentially expressed genes were clustered using Cluster 3.0 and visualized with Java TreeView [35]. GO terms and KEGG pathway enrichment were analyzed using DAVID version 6.8 [36,37]. Volcano plots were created using R version 3.5.1. Over-represented transcription factor-binding sites were detected by mouse single-site analysis with default settings using oPOSSUM version 3.0 [38]. Next, 10,000 bp upstream and downstream of the transcription start site of the genes that were expressed (normalized counts > 50) at the respective time points were used as background.

2.13. Gene set enrichment analysis

Gene set enrichment analysis (GSEA) (http://www.broad.mit.edu/GSEA) [39,40] was performed with 1,000 permutations and a weighted enrichment statistic. For GSEA used to identify differentially enriched GO terms and pathways at 32 weeks, all of the expressed genes (13,906 genes) were ranked by their -$\log_{10}$ (adjusted P value) x ($\log_2$FoldChange) estimated by DESeq2. Gene sets smaller than 5 and larger than 200 were excluded from the analysis. Gene set Mouse_-GO_AllPathways_no_GO_iea_January_01_2020_symbol compiled by the Bader Lab at http://download.baderlab.org/EM_Genesets was used for the GSEA. Cytoscape was used for network visualization [41] with Enrichment Map [42] and AutoAnnotate [43] plugins as previously described [44]. All labels were edited for simplicity.

For GSEA used for comparisons with established models of cardiac stress and human hearts affected by disease, gene sets were generated *de novo* by analyzing publicly available raw RNA-seq data: SRP076218 (isoproterenol-induced stress) [45], SRP055928 (TAC) [46], E-MTAB-727 (exercise-induced hypertrophy) [47], SRP055875 (diabetic cardiomyopathy) [48], SRP093239 (Ang-II induced hypertension), SRP186138 (hypertrophic cardiomyopathy) [49], and SRP151309 (dilated and ischemic cardiomyopathy) [50]. The specific samples analyzed from each study are shown in Table S1. For each model, the differentially expressed genes were categorized as up- or downregulated. All the genes that were differentially expressed in the adult hearts ($P < 0.05$) were used as input in a pre-ranked gene list to conduct a more focused analysis given that the gene sets used for input were based only on differentially expressed genes. Genes were pre-ranked by their -$\log_{10}$ (adjusted P value) x ($\log_2$ fold change) estimated by DESeq2. 1000 permutations were conducted using a weighted statistic. The complete sets of genes that were differentially expressed in the different models and human hearts affected by disease were used for the analysis, so a gene set size limit was not established. GSEA was performed using databases of the up- and downregulated genes, separately. We focused on genes with positive enrichment scores when using the upregulated gene set database and negative enrichment scores when using the downregulated gene set to determine similarity, that is, models with the highest direct correlation with genes differentially expressed in our model.

2.14. Gene network analysis

GeneMania [51] was used to build the networks used for the focused analysis of individual pathways. Interactions were visualized using

 © 2020 The Authors. Published by Elsevier GmbH. This is an open access article under the CC BY-NC-ND license (http://creativecommons.org/licenses/by-nc-nd/4.0/).

Cytoscape [41]. Gene lists used as input representing the different pathways were manually curated from differentially expressed genes by combining KEGG pathways and GO terms related to the respective pathways. The full list of terms used for manual curation is provided in Table S4.

2.15. Phenotypic correlation with gene expression

Normalized gene expression levels were correlated with phenotypic variables using Pearson's correlation test. The Benjamini and Hochberg correction was applied to correct for multiple tests. This was repeated using 10,000 size-matched sets of genes randomly selected from the universe of all the expressed genes. The bootstrap *P* value was reported as the number of permutations with the number of significantly correlated genes $\geq$ the number observed for DEGs.

2.16. ChIP-seq analysis

ChIP-seq data for Nkx2-5 in the adult hearts was obtained from GSE35151 [52], in cardiac progenitors from GSE77548 [16], and in human cardiac cells from GSE89457 [53]. Bed files of Nkx2-5 peaks were obtained from these studies and Nkx2-5 bound genes were determined with the Genomic Regions Enrichment of Annotation Tool (GREAT) [54] version 4.0.4 mm9 or hg19 assembly using the default settings. Fisher's exact test was used to determine enrichment. Differentially expressed genes were defined by an adjusted *P* value < 0.05. Genes whose expression did not significantly change and that were used for the test were defined as all the expressed genes with a mean expression greater than that of the lowest differentially expressed gene at the respective time point. Bigwigs used to generate the aggregate plots were obtained from GSE35151 [52] and GSE77548 [16].

2.17. Statistical analysis

Data are presented as the mean $\pm$ S.E.M. unless otherwise indicated. Two group comparisons were conducted using Student's t-test. ANOVA was used for multiple group comparisons or comparisons of 2 groups over time. Multiple hypothesis testing correction was performed as indicated in the manuscript and Tables S2 and S3. $P < 0.05$ was considered significant. Statistical analyses were conducted either using GraphPad Prism 6 or R.

3. RESULTS

3.1. Maternal high-fat diet programs progressive heart dysfunction in adult offspring

To determine the contribution of maternal obesity to heart disease predisposition in the offspring, we fed the female mice a control diet (CD) or a mildly obesogenic high-fat/high-sugar diet (HD) (Figure S1). The HD induced significant weight gain (Figures S2A and S2B) due to increased fat deposition (Figure S2C). However, the HD did not alter glucose tolerance in the dams (Figure S2D). Females at $\sim$20 weeks of age were mated with CD-fed males and the offspring were weaned to a CD. Male offspring born to the females fed the HD (referred to as OH) had a small increase in weight that was due to an increase in both fat and lean mass (Figures S3A and S3B). Body fat percentage was also increased and lean percentage decreased in the OH (Figure S3B). However, glucose tolerance was comparable between the OH and offspring born to the CD-fed females (referred to as OC) at 8 and 32 weeks of age (Figure S3C). This suggested that the HD induced weight gain with limited metabolic dysfunction in the female mice and their offspring.

To examine the effect of obesity during pregnancy on heart function in the adult offspring, echocardiography was performed on the OC and OH at 16 and 32 weeks of age. At 16 weeks, the OH had a reduced peak E/A ratio concomitant with a longer isovolumetric relaxation time (IVRT, normalized to cardiac cycle length) (Figure 1A–C and Figure S4A), indicating reduced diastolic function. In contrast, ejection fraction and fractional shortening were not altered, indicating normal systolic function (Figure 1D,E). Heart function deteriorated at 32 weeks of age in the OH. Both the ejection fraction and fractional shortening were reduced (Figure 1D,E). This systolic dysfunction was coupled with normalization of the peak E/A ratio (Figure 1B), which is known to occur during the progression of diastolic dysfunction [55]. In addition, the heart mass was mildly increased (Figure 1F) with a corresponding increase in the cell surface area of apical ventricular cardiomyocytes (Figure 1G,H and Figure S4B), indicating localized cardiomyocyte hypertrophy. The heart rate was significantly reduced in the OH (Figure 1I), a known risk factor for heart disease [56]. Notably, the longer IVRT, a $\sim$10% reduction in ejection fraction, and a $\sim$5% reduction in fractional shortening in OH were mild and likely representative of early subclinical stages of heart disease. Accordingly, fibrous tissue infiltration was not increased in the hearts of the OH (Figure S4C). Only *S100a4* and *Myh6*, but not *Myh7*, *Nppa*, *Nppb*, *Acta1*, or *Gata4*, often deregulated in hearts affected by disease [57], were abnormally expressed in the hearts of the OH (Figure S4D). Thus, the maternal HD led to a subtle and progressive decline in cardiac function consistent with subclinical heart disease.

3.2. Obesity during pregnancy dysregulates transcriptional pathways underlying heart dysfunction

To ascertain the transcriptional pathways underlying heart dysfunction programmed by obesity during pregnancy, we analyzed the genome-wide mRNA profile of adult ventricles in the OH and OC at 32 weeks of age by RNA-seq. The mRNA expression profile of ventricles of OH clustered separately from OC in a principal component analysis (PCA), indicating distinct transcriptional profiles (Figure 2A). Differential expression analysis identified 1,372 significantly dysregulated genes (adjusted *P* value < 0.05), of which 485 were upregulated and 887 downregulated in the OH (Figure 2B). The expression levels of 98% (1,338) of the genes dysregulated in the OH changed by less than two-fold (Figure 2C), suggesting that small but broad changes in gene expression underlie subclinical heart dysfunction.

Gene ontology (GO) analysis revealed that genes upregulated in the adult heart of the OH were most highly enriched for terms related to ECM remodeling and collagen organization. Terms related to inflammatory response, fibroblast proliferation, and TGF-β signaling were also significantly enriched (Figure 2B). The PI3K-Akt signaling pathway, which is activated downstream of TGF-β [58] and was previously found to be overactivated in the adult heart in response to obesity during pregnancy [8], was among the top 5 upregulated pathways identified by our analysis (Figure 2D).

Consistent with a reduced heart rate in the adult OH (Figure 1I), regulation of the heart rate was among the top enriched GO terms in downregulated genes (Figure 2B). KEGG pathways related to metabolism, such as insulin signaling and downstream MTOR and AMPK, signaling were the most highly enriched downregulated pathways (Figure 2D). Accordingly, network maps of the GSEA showed higher expression of ECM and inflammation-related gene sets and lower expression of genes in the cardiac contraction, insulin, and metabolic pathways as well as cardiac development-related gene sets (Figure S5A). qPCR on the ventricles of the OH confirmed the

 © 2020 The Authors. Published by Elsevier GmbH. This is an open access article under the CC BY-NC-ND license (http://creativecommons.org/licenses/by-nc-nd/4.0/).

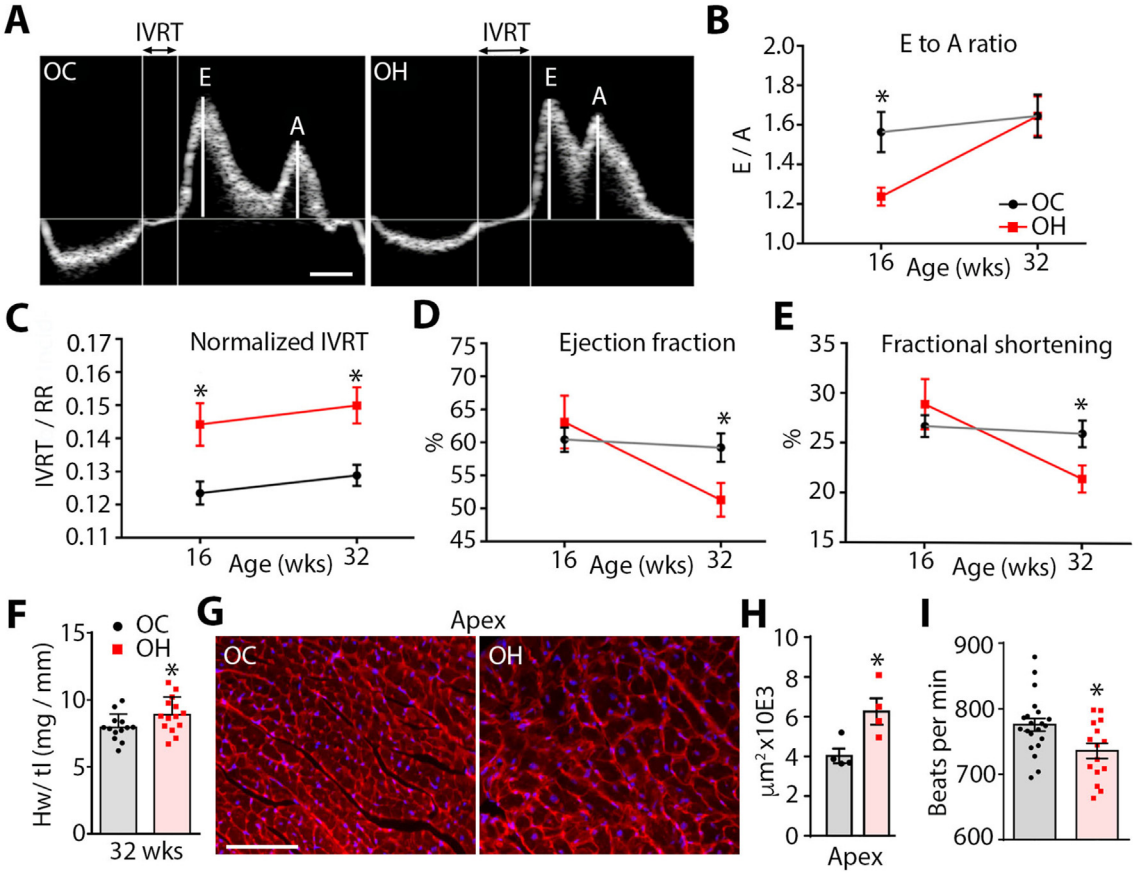

Figure 1: Cardiac dysfunction progressed with age in male offspring born to obese mice. (**A**) Representative pulsed Doppler recording of blood flow across the mitral valve for a cardiac cycle in mice born to females fed a control (OC) or high-fat diet (OH) at 16 weeks. Isovolumetric relaxation time (IVRT) is indicated between the white lines. Peak velocities of early (E) and late/atrial (A) diastolic filling waves are highlighted. Scale bar = 20 msec. (**B**) Peak E to A ratios at 16 and 32 weeks. (**C**) IVRT normalized to the length of the cardiac cycle (RR). (**D**) Left ventricular ejection fraction of the OH and OC at 16 and 32 weeks. (**E**) Left ventricular fractional shortening of the OH and OC at 16 and 32 weeks. For **B** to **E** N = 7–8 mice per group at each time point. (**F**) Heart weight normalized to the tibia length ratio in the OH and OC. N = 13–14 mice per group. (**G**) Wheat germ agglutinin staining on sections of the apex of the heart. Scale bar represents 100 µm. (**H**) Cell surface area in sections of the heart apex. N = 4 mice per group. (**I**) Heart rate of the unanesthetized OH and OC. N = 21 and 15 mice per group. Student's t-test. Bars represent the mean ± SEM.

upregulation of *Col3a1*, *Col6a3*, *Fbn1*, and *MMP14*, which are key regulators of ECM assembly and turnover, genes in the TGF-β pathway *Thbs1* and *Tgif1*, and the pro-inflammatory gene *Egfr*. qPCR also confirmed downregulation of the ion channel *Scn5a* and the metabolic regulator *AKT1* (Figure 2E). Thus, upregulation of genes controlling ECM, inflammation, and TGF-β signaling and concomitant downregulation of metabolic regulators of insulin signaling and downstream MTOR and AMPK pathways defined subclinical heart dysfunction in the OH.

To more precisely define the context of heart dysfunction in the offspring born to the obese mice, we compared the expression profile in hearts of the OH against publicly available expression profiles of several mouse models of cardiac stress and human hearts affected by disease. We analyzed mouse models of angiotensin II-induced hypertension, diabetic cardiomyopathy, chronic isoproterenol (ISO)-induced adrenergic stimulation, transverse aortic constriction, and physiological hypertrophy. Human hearts with dilated cardiomyopathy, hypertrophic cardiomyopathy, and ischemic cardiomyopathy were also analyzed (Table S1). The transcriptional profile of hearts of the OH at 32 weeks of age was most similar to the hearts of mice with diabetic cardiomyopathy and isoproterenol-induced adrenergic stimulation, followed by hypertrophic cardiomyopathy (Figure S5B). Indeed, as in the OH hearts, the expression of ECM components and insulin signaling regulators was perturbed in the diabetic mouse model [59]. In addition, diabetic cardiomyopathy had a long latent phase in which the heart was mildly hypertrophied, stress marker genes and ECM components were expressed normally, and early signs of diastolic dysfunction progressed to systolic dysfunction [59]. Moreover, ECM deposition and inflammation increased in hypertrophic cardiomyopathy and models of ISO-induced stress [60,61].

GSEA using the genes that were up- and downregulated in the heart of each of the 8 models also revealed that gene sets related to diabetic, hypertrophic, and ISO-induced cardiomyopathy were enriched in genes dysregulated in the OH (Figure 2F). This gene dysregulation was not secondary to hypertension or diabetes because blood pressure and glucose tolerance were not significantly different between the OC and OH (Figures S6 and S3C). Thus, mild dysregulation of genes in pathways controlling the response of the heart to stress and pathological remodeling in OH revealed a state of preclinical heart dysfunction. Linking such transcriptional signatures to specific phenotypes in the pregnant obese mice and OH revealed potential predictors of heart disease risk in the offspring.

 © 2020 The Authors. Published by Elsevier GmbH. This is an open access article under the CC BY-NC-ND license (http://creativecommons.org/licenses/by-nc-nd/4.0/).

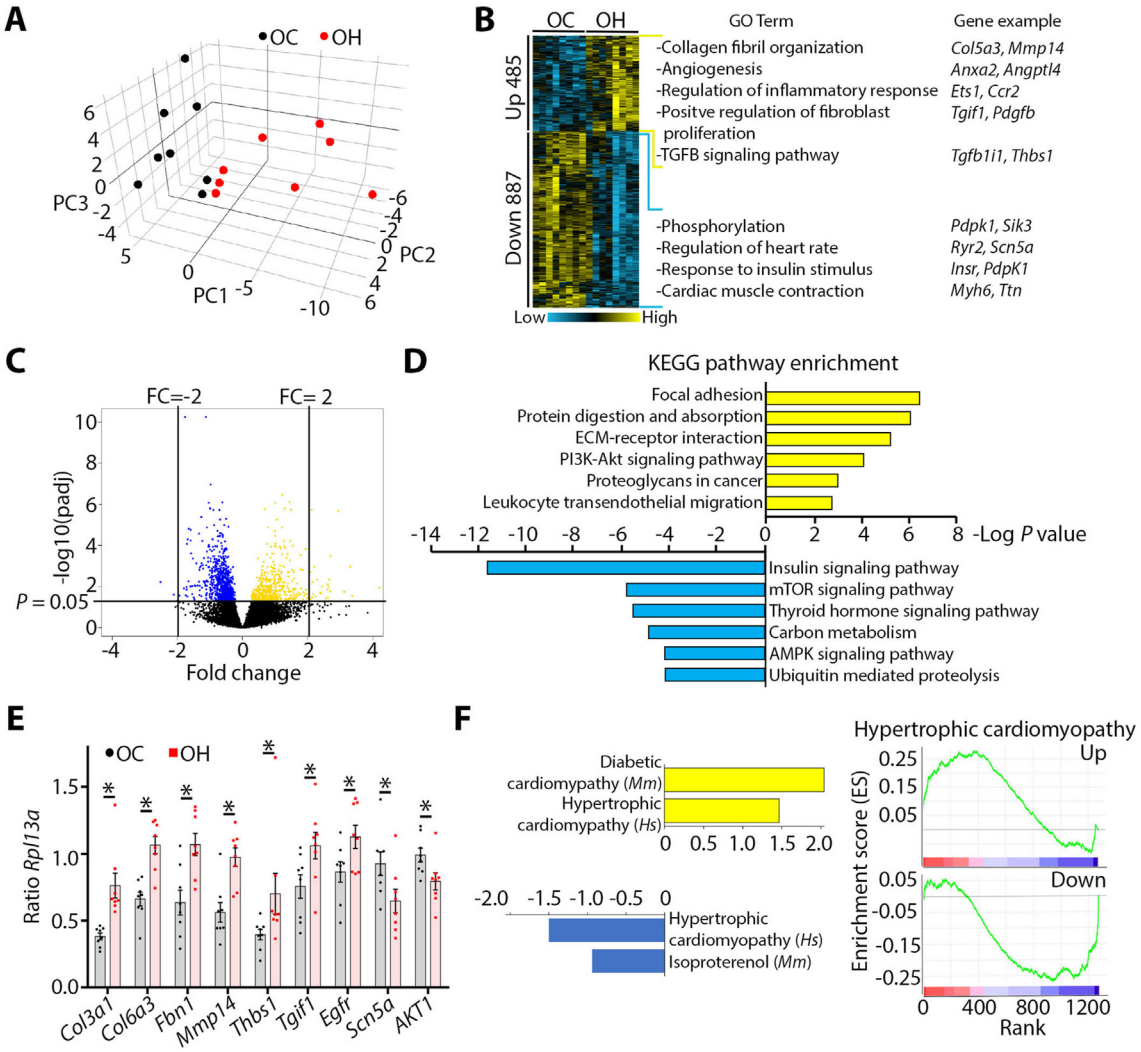

Figure 2: Higher maternal weight was associated with small but broad changes in transcriptional pathways controlling heart disease. (**A**) Principal component analysis (PCA) plot displaying separation of cardiac transcriptomes by maternal diet. (**B**) Heatmap clustering of differentially expressed genes between ventricles of the OH and OC at 32 weeks of age. Enriched GO terms and representative genes are shown on the right. (**C**) Volcano plot of all the detected genes. Significantly downregulated genes are in blue and upregulated in yellow. (**D**) KEGG pathways enriched in genes that were significantly up- and downregulated in mice born to obese mice. (**E**) qPCR on hearts of the OC and OH at 32 weeks. The genes analyzed are representative of the pathways identified in (**B**). N = 8 mice per group. (**F**) Gene set enrichment analysis of hearts affected by different diseases compared to genes up- and downregulated in our model. Positively and negatively enriched gene sets are on the left, enrichment plots of hypertrophic cardiomyopathy, one of the top enriched terms, are on the right. Bars represent the mean ± SEM.

3.3. A high maternal weight, an increased heart weight, and a longer IVRT in the offspring predict a state of subclinical heart disease

To identify traits associated with the transcriptional signature of hearts and subclinical heart dysfunction, we analyzed the correlation between differentially expressed genes in the heart of the OH or 10,000 permutations of randomly selected genes as controls against the maternal and offspring phenotypes. Of 55 total phenotypic parameters (Table S2), variations in 10 phenotypes significantly corelated with variability in differentially expressed genes (Figures 3A and S7). Forty-five phenotypic parameters, including the percentage of fat and lean mass of the offspring, did not correlate with gene expression changes, excluding such phenotypes as potential drivers of gene dysregulation in the heart (Table S2). Notably, maternal weight at the time of conception correlated with the largest number of differentially expressed genes. The mRNA levels of 1,135 of the 1,372 differentially expressed genes (83%) significantly correlated with maternal weight as a continuous variable (range 21.1—29 g) (Figure 3A and Table S2). Accordingly, PCA showed that distinct transcriptional profiles were associated with higher maternal weights (Figure 3B).

Closer examination of differentially expressed genes in the most highly enriched pathways revealed that a higher maternal weight correlated with predominant upregulation of ECM components and downregulation of insulin and heart rate regulators (Figure 3C). A higher heart weight in the OH correlated with a lower expression of genes in the insulin signaling pathway, for example, *PPARα*, whose deficiency promotes cardiac hypertrophy [62] and less with dysregulated ECM components (Figure 3D). A longer IVRT was the phenotype in the OH that significantly correlated with the largest number of differentially expressed genes (Figure 3A), including upregulation of ECM components *Col1a2* and *Col6a2* (Figure 3E), which is associated with increased stiffening of the ventricular wall

 © 2020 The Authors. Published by Elsevier GmbH. This is an open access article under the CC BY-NC-ND license (http://creativecommons.org/licenses/by-nc-nd/4.0/).

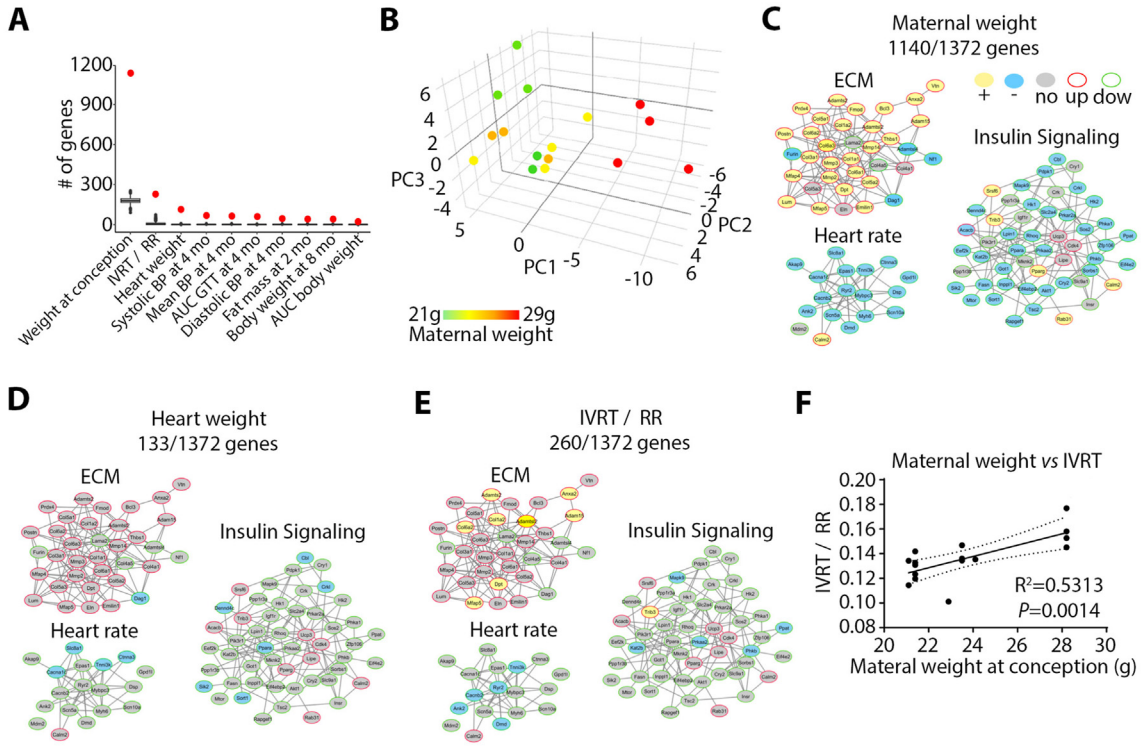

Figure 3: Maternal weight and several cardiac phenotypes correlated with dysregulation of specific pathways in the heart. (**A**) Number of genes that significantly correlated with various maternal and offspring phenotypic parameters. Red dots represent the observed number of differentially expressed genes correlated with each phenotype (bootstrap P value < 0.05). Box plots depict 10,000 permutations of randomly selected genes. (**B**) Principal component analysis of transcriptomes separated by maternal weight at conception. (**C**) Gene network displaying all the differentially expressed genes in the top three enriched processes (ECM, heart rate regulation, and insulin signaling). Genes that correlated with maternal weight are highlighted. (**D**) Networks highlighting differentially expressed genes that correlate with heart weight and (**E**) isovolumetric relaxation time corrected to the time between heartbeats (IVRT/RR). no = genes whose expression did not change, up = genes upregulated, and down = genes downregulated in the OH compared to OL. Positive (+) and negative (−) correlations refer to a significant Pearson's correlation (adjusted $P < 0.05$) of gene expression levels and the respective phenotype after Benjamini and Hochberg correction for multiple tests. (**F**) Pearson's correlation between maternal weight at conception and IVRT/RR.

[63,64]. Furthermore, IVRT positively correlated with maternal weight (Figure 3F). Thus, a higher maternal weight, followed by a longer IVRT and higher heart weight, was the strongest predictor of dysregulation of genes controlling pathological remodeling in preclinically dysfunctional hearts in the OH.

3.4. Offspring of obese dams develop exacerbated myocardial remodeling in response to stress

To test whether obesity during pregnancy increased heart disease susceptibility in the offspring, we induced pathologic stimulus in 2-month-old OH before the onset of cardiac dysfunction. The OC and OH were infused with PBS or ISO for two weeks using osmotic pumps. Before ISO treatment, heart morphology and function were comparable between the OC and OH (Table S3). In response to ISO-induced stress, the ventricular walls of the OC and OH significantly thickened (Figure 4A and Table S3). In response to ISO, the OH developed a more severe constriction of the ventricular diameter at end systole and diastole (Figure 4B,C). Similarly, chamber volumes at end diastole and cardiac output decreased in the OH compared to the OC (Figure 4D,E), suggesting exacerbated restrictive hypertrophy. Systolic and stroke volumes tended to decrease in the OH (Figure S8). Unlike the OC, the OH failed to shorten the IVRT in response to ISO infusion (Figure 4F), suggesting impaired diastolic function. Moreover, collagen deposition was exacerbated in the OH treated with ISO (Figure 4G,H). This indicated that under basal conditions, young 2-month-old OH had normal cardiac morphology and function but were poised for dysregulated stress responses.

To ascertain the processes mediating an exacerbated response to stress in the OH, we compared the transcriptome of hearts of 2-month-old OC and OH that were stressed with ISO or treated with PBS. A PCA separated the groups of ISO- and PBS-treated mice in component 1, which explained the largest proportion of variations (Figure 4I). PBS-treated and more distinctively ISO-treated hearts were separated by maternal diet on principal component 2 (Figure 4I). Among the top 50 genes that explained the largest proportion of principal component 2, regulators of inflammation (e.g., *Nr4a1* and *Igtp*) and ECM components (e.g., *Fbn1*) were overexpressed in the OH (Figure 4J). Accordingly, genes controlling inflammation and ECM components were upregulated in the OH treated with PBS or ISO (Figure 4K). Unsupervised clustering of the genes that were differentially expressed between the OC and OH treated with PBS or ISO revealed dynamic stress responses (Figure 4L). Similar to untreated 32-week-old hearts of the OH (Figure 2B,D), genes upregulated in the OH at 10 weeks of age (clusters 1−4) were enriched for GO terms related to ECM and heart development, while downregulated genes (clusters 5−8) were enriched for GO terms related to metabolism and negative regulation of BMP/TGF-β (Figure 4L). Subsets of these genes responded differently to ISO. For example, some genes were upregulated in the PBS-treated OH and remained upregulated (cluster 2) or were downregulated (cluster 4) in response to ISO (Figures 4L and S9). Notably, genes

 © 2020 The Authors. Published by Elsevier GmbH. This is an open access article under the CC BY-NC-ND license (http://creativecommons.org/licenses/by-nc-nd/4.0/).

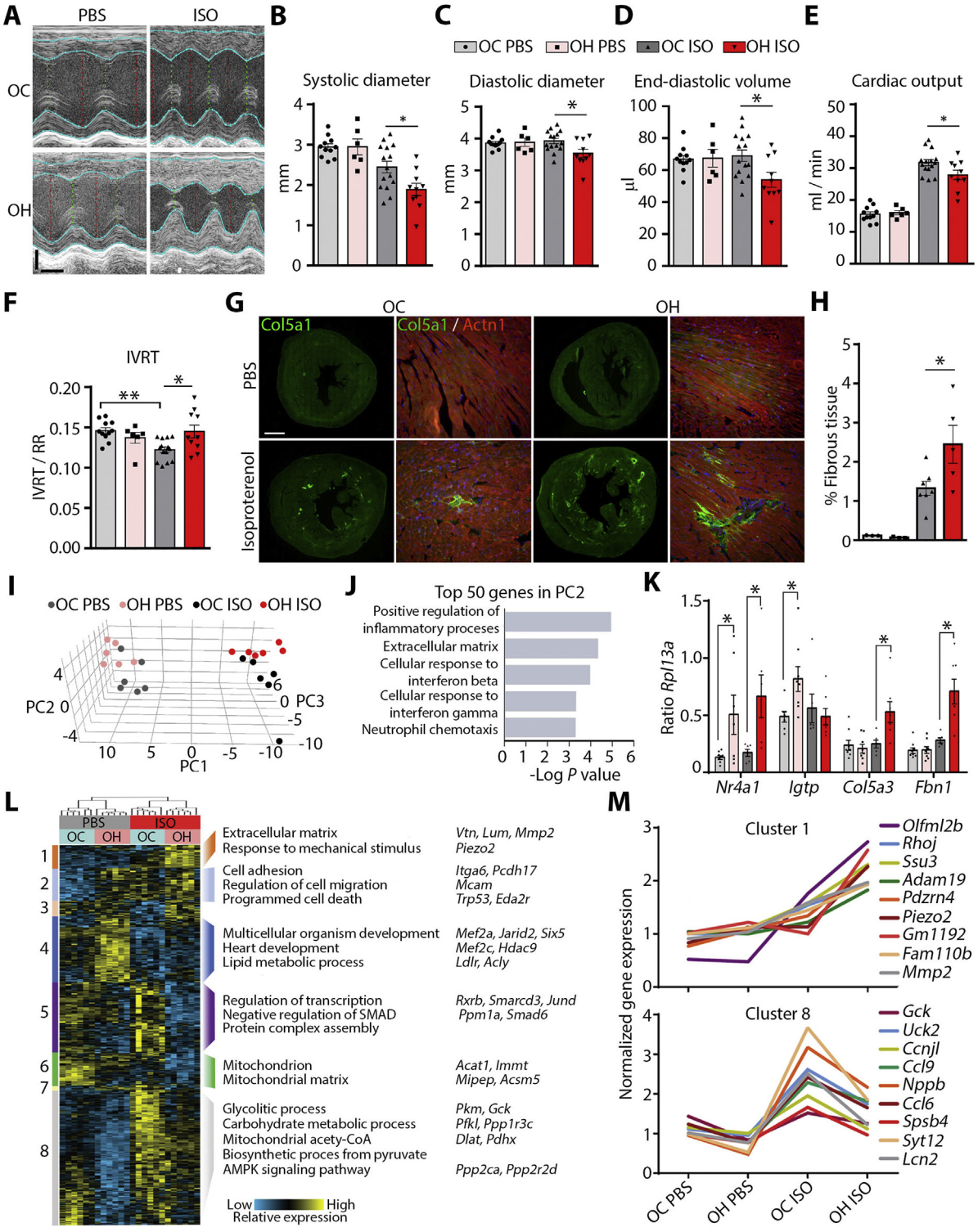

Figure 4: Male offspring of HD developed exacerbated pathological remodeling in response to isoproterenol infusion. (**A**) M mode echocardiogram of the left ventricle of mice born to females fed a control (OC) or high-fat diet (OH) that were treated with PBS or isoproterenol (ISO). Horizontal scale bar = 50 msec and vertical scale bar = 1 mm. (**B**) End systolic diameter. (**C**) End diastolic diameter. (**D**) End-diastolic volume. (**E**) Cardiac output. (**F**) Isovolumetric relaxation time normalized to the time between heartbeats (IVRT/RR). For **B** to **F**, N = 11, 6, 15, and 10 mice per group, respectively. One-way ANOVA. (**G**) Immunofluorescence against collagen type V alpha 1 (Col5a1) and actinin alpha 1 (Actn1). (**H**) Quantification of fibrosis area percentage. N = 3, 3, 7, and 5 mice per group, respectively. (**I**) Principal component (PC) analysis plot separated cardiac transcriptomes by treatment on PC1 and maternal diet on PC2. (**J**) GO term enrichment for the top 50 genes determining PC2. (**K**) qPCR of representative genes on PC2 in (**I**). Bars represent the mean ± SEM. N = 6–8 mice per group. (**L**) Unsupervised hierarchal clustering of genes that were differentially expressed between ventricles of the OH and OC treated with PBS or ISO at 10 weeks of age. Enriched GO terms and representative genes are shown on the right. (**M**) Expression profiles (magnitude of normalized count values) of gene clusters 1 and 8. Bars represent the mean ± SEM. One-way ANOVA with Tukey's multiple comparisons was used to determine the *P* values.

 © 2020 The Authors. Published by Elsevier GmbH. This is an open access article under the CC BY-NC-ND license (http://creativecommons.org/licenses/by-nc-nd/4.0/).

enriched in ECM components were most highly upregulated in the OH in response to ISO (cluster 1). Moreover, genes enriched for mitochondria and metabolism-related GO terms were strongly upregulated in the OC and to a lesser extent in the OH in response to ISO (cluster 8) (Figure 4L and M and Figure S9). These results suggested that obesity during pregnancy sensitized the heart to overexpression of ECM components and attenuated activation of metabolic regulators to program dysregulated stress responses in the heart.

3.5. Pathways controlling heart disease are dysregulated in differentiating embryonic CPs in response to obesity during pregnancy

Disrupting key transcriptional pathways in differentiating CPs during embryogenesis leads to adult-onset heart disease [24]. To ascertain the embryonic origins of adult heart disease susceptibility in the OH, we analyzed the mRNA profiles of differentiating CPs in E9.5 embryos of the mice fed a HD or CD by RNA-seq. CPs were sorted from embryos carrying an *Nkx2-5-eGFP* transgene [25], which labeled CPs of the first and second heart fields at E9.5 (Figure S10A). CPs were isolated from individual embryos of dams fed CD and HD and spanning a narrow weight range between 23 and 26 g. The eGFP-positive cell fraction was enriched in CPs, which expressed higher levels of CP marker genes *Nkx2-5* and *Isl1* compared to eGFP-negative cells (Figures S10B and C). Gene expression analysis of CPs from the embryos of dams across all the weights identified only 9 genes that were differentially expressed in response to a HD (Figure 5A). This suggested that a maternal HD per se did not lead to altered global gene expression in differentiating CPs.

BMI in humans proportionally correlates with the risk of cardiovascular disease and mortality in offspring [2–4]. This is consistent with a higher maternal weight correlating with a greater number of dysregulated genes in hearts of the OH (Figure 3A). Indeed, a focused comparison of CPs from embryos of the leanest CD-fed dams against the heaviest HD-fed dams revealed a significantly broader effect on gene expression. A total of 823 genes were dysregulated, of which 586 were upregulated and 237 downregulated (Figure 5B). Upregulated genes were most highly enriched for ontologies related to heart development. TGF-β signaling and ECM organization were also among highly enriched terms (Figure 5B). KEGG pathways related to hypertrophic, dilated, and arrhythmogenic cardiomyopathy were among the most significantly enriched terms (Figure 5C). In contrast, downregulated genes were enriched for epigenetic processes including nucleosome assembly and DNA methylation (Figure 5B), suggesting potential mechanisms of gene dysregulation.

3.6. *Nkx2-5*-controlled transcription is dysregulated in CPs of embryos of obese dams

Maintaining core transcription networks in CPs and their descendants is required for cardiogenesis and stable long-term postnatal heart function [16,24]. We sought to identify genes and pathways that were perturbed in CPs and persistently into adulthood. A total of 112 genes were commonly dysregulated in embryonic CPs and adult hearts from the OH (Figure 5D). These genes were enriched for functions directly related to heart disease, including hypertrophic cardiomyopathy, ECM-receptor interactions, and metabolism (Figure 5D). This suggested that the deregulation of genes controlling heart disease in the OH was programmed in developing CPs. To ascertain transcription factors controlling heart disease risk, we searched for binding motifs enriched in the regulatory region of genes dysregulated in the heart of the adult OH and CPs. The Nkx2-5 binding motif was the most enriched in the 10 kb 5′ upstream and 3′ downstream of the transcription start site (Figure 5E) and was present in all 112 genes that were dysregulated commonly in CPs and adult hearts of the OH (Figure S11). In addition, *Nkx2-5* was downregulated in CPs of embryos from the HD-fed dams (Figure 5F). Furthermore, *Nkx2-5* transcript levels negatively correlated with the dams' weights (Figure 5G). To determine whether these genes were directly bound by Nkx2-5, we analyzed published Nkx2-5 ChIP-seq datasets from differentiating CPs [16] and adult mouse hearts [52]. We found that genes differentially expressed in response to maternal obesity in the hearts of the OH were enriched for direct Nkx2-5 targets (Figure 5H–J). Nkx2-5 targeted both upregulated and downregulated genes in CPs and adult hearts (Figure 5H–J). However, Nkx2-5 preferentially targeted genes upregulated in CPs and genes downregulated in adult hearts (Figures 5K and 5L), consistent with functions of Nkx2-5 as both an activator and repressor of gene expression [16,52,53].

3.7. Maternal BMI correlates with altered expression of genes controlling mitochondrial metabolism, ECM-cell interactions, and cell adhesion in the human fetal heart

To ascertain the effect of obesity during pregnancy on the human fetal heart, we performed RNA-seq on the ventricles of 53 fetuses from healthy (BMI 18.6–24.9 kg/m^2), overweight (BMI 25.0–29.1 kg/m^2), and obese (BMI 30.2–49.6 kg/m^2) donors at a gestational age between 8 and 19 weeks. Ventricular septation is almost complete by 8 weeks, which was the earliest time point when collection was possible. PCA separated the samples by gestational age on PC1 and sex on PC2, which explained 42% and 19% of variations, respectively (Figure S12A). Similarly, heatmap clustering by Euclidean distance identified 4 main groups largely defined by gestational age (Figure S12B). Group 1 comprised hearts from 8 to 9.9 weeks of gestation. Groups 2, 3, and 4 spanned more broadly from 10 to 12.9, 13 to 15.9, and 16–18.5 weeks, respectively. Expression of only 3 genes significantly corelated with BMI as a continuous variable: *GALNT14*, a protein glycosyltransferase, and two pseudogenes *PRSS46P* and *MTATP8P1* (Figure S12C). Similarly, expression of 3 genes was significantly associated with obesity as a categorical variable: *MTRNR2L12*, *MTRNR2L1*, and *MTCO3P12* (Figure S12D), all of which are encoded in the mitochondrial genome. This suggested that obesity *in utero* did not broadly alter gene expression in the human fetal heart independently of sex and age.

Overlapped pathways but different genes were dysregulated in CPs and adult mouse hearts born to obese mice (Figures 2, 4 and 5). Therefore, we stratified the human fetal transcriptomes by gestational age into two groups, one from 8 to 9.4 weeks (14 samples) and another from 15.3 to 16.6 weeks (9 samples). Hearts in these groups were very similar at the global gene expression level but came from donors spanning a broad BMI range (Figure S12A and B). In hearts at 8–9.4 weeks of gestation, the expression of 128 genes increased and 76 decreased per unit increase in BMI (referred to as Early-Cor) (Figure 6A). Positively corelated genes were enriched for functions related to increased lipid metabolism and mitochondrial function such as electron transport and mitochondrial translation (Figure S13A). These genes include aldehyde dehydrogenase (*ALDH2*), which is a major enzyme in oxidative metabolism of aldehydes, and NADH dehydrogenase 3 (*MT–ND3*), which promotes electron transport in the mitochondria. Genes whose expression decreased with every increase in BMI were enriched for terms related to cell adhesion and muscle development (Figure S13A). For example, the expression of filamins A and C, which anchor membrane proteins to actin filaments and maintain muscle integrity [65], decreased as BMI increased. Analysis of hearts between 15.3 and 16.6 weeks of gestation identified 83

 © 2020 The Authors. Published by Elsevier GmbH. This is an open access article under the CC BY-NC-ND license (http://creativecommons.org/licenses/by-nc-nd/4.0/).

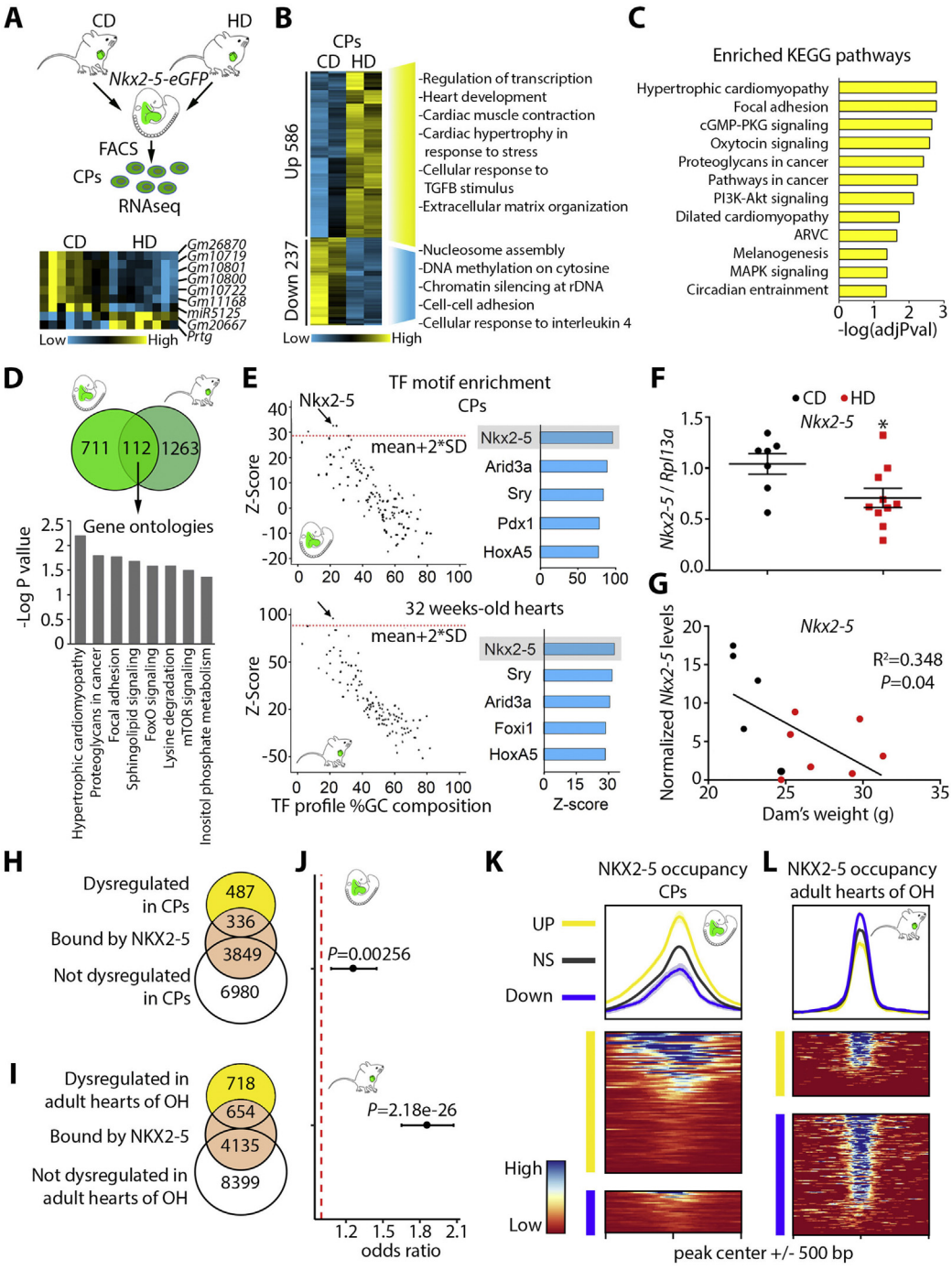

Figure 5: Maternal obesity induced dysregulation of Nkx2-5 target genes in cardiac progenitor cells and persistently in adult hearts. (**A**) Cardiac progenitor cells (CPs) were isolated by fluorescence-activated cell sorting (FACS) from embryos of dams carrying an *Nkx2-5-eGFP* transgene and that were fed a control (CD) or high-fat (HD) diet. CPs were used for RNA-seq. The heatmap represents the mRNA levels of 9 genes differentially expressed in CPs of embryos from the HD-fed mice. (**B**) Heatmap of genes dysregulated in CPs of embryos of the heaviest vs leanest mice. (**C**) KEGG pathways enriched in the dysregulated genes. (**D**) Venn diagram of genes dysregulated in CPs and adult (32 weeks) hearts and enriched ontologies in commonly dysregulated genes. (**E**) Motif enrichment analysis of genes dysregulated in CPs (top) and adult hearts (bottom). (**F**) qPCR of *Nkx2-5* in CPs of embryos from the CD- and HD-fed mice. Each dot represents CPs from an individual embryo. Bars represent the mean ± SEM. N = 7 and 10, respectively. Student's t-test was used to determine the *P* values (**G**) Pearson's correlation analysis of *Nkx2-5* mRNA in CPs vs maternal weight. Each dot represents pooled CPs from embryos from one litter. N = 5 and 7, respectively. (**H**) Number of genes with Nkx2-5-bound regions (determined using GREAT version 4.0.4 mm9 assembly) in CPs and (**I**) adult hearts. (**J**) Fraction of differentially expressed genes bound by Nkx2-5 compared to the fraction expected by chance for the overlaps in (**H**) and (**I**). Bars show 95% confidence intervals. Odds ratio and *P* value were obtained using Fisher's exact test. (**K**) Nkx2-5 ChIP-seq peaks proximal to differentially expressed genes in CPs and (**L**) adult hearts. Aggregate plots (top) show the mean ± SEM of signals in each category. Heatmaps show the Nkx2-5 signal centered on the TSS of genes lacking a promoter proximal peak. Up = upregulated, down = downregulated, and NS = not significantly changed. Only genes on the list used by GREAT were included in (**H**)–(**L**).

 © 2020 The Authors. Published by Elsevier GmbH. This is an open access article under the CC BY-NC-ND license (http://creativecommons.org/licenses/by-nc-nd/4.0/).

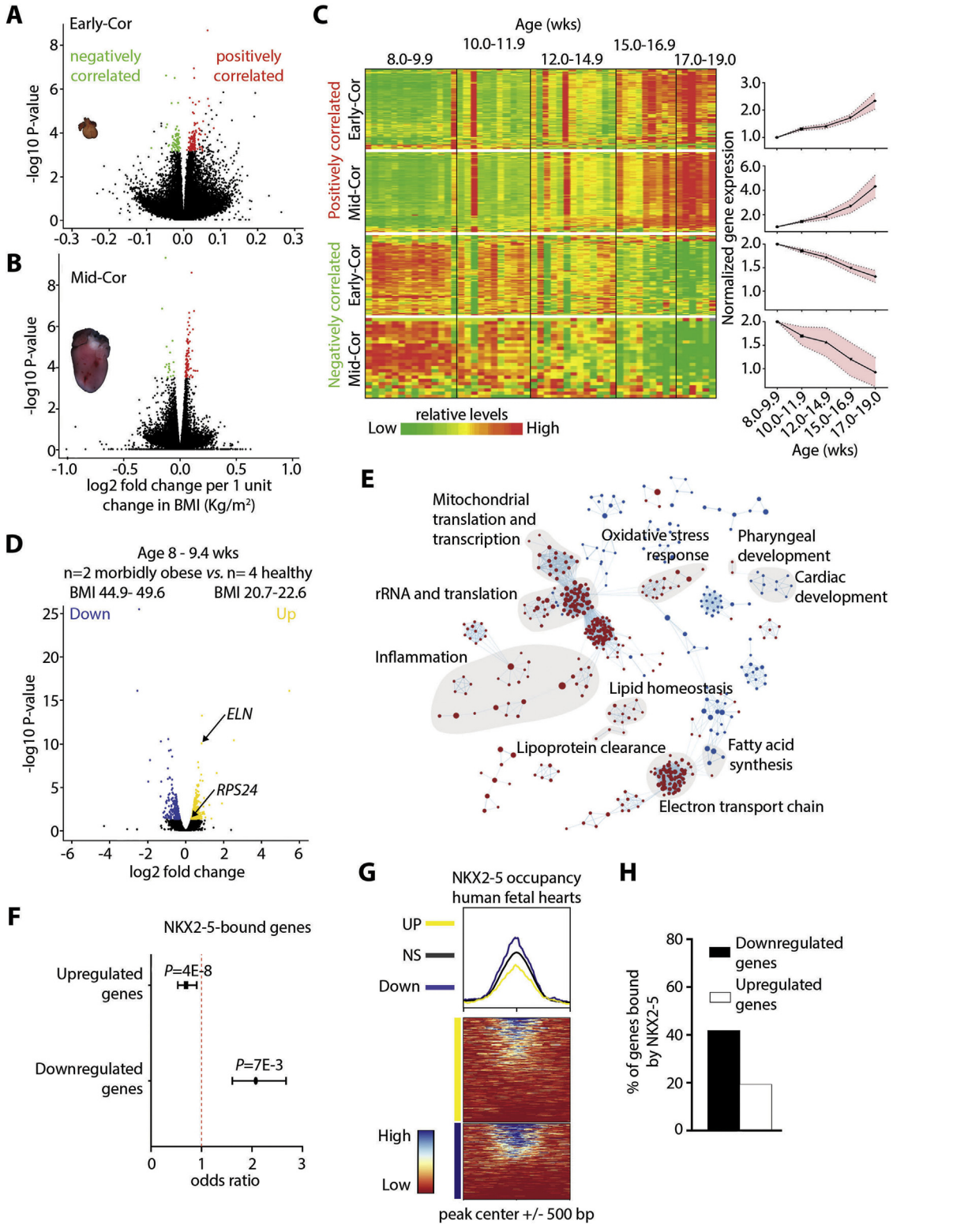

Figure 6: Nkx2-5 targeted genes abnormally expressed in human fetal hearts in response to exposure to obesity *in utero*. (**A**) Volcano plot of all the expressed genes in 8- to 9.4-week-old hearts. Genes that are significantly downregulated per unit increase in BMI are in green, and upregulated genes are in red. (**B**) Volcano plot of all the expressed genes in 15.3- to 16.6-week-old hearts. (**C**) Heatmap showing gene expression level of Early and Mid-Cor genes in human fetal hearts at different developmental stages. Normalized gene expression is shown on the right. (**D**) Volcano plot of all of the expressed genes in 8- to 9.4-week-old hearts of fetuses of morbidly obese vs healthy donors. Upregulated genes are in yellow and downregulated genes are in blue. (**E**) Network clustering showing gene sets (from GSEA) enriched in upregulated (red) and downregulated (blue) genes. (**F**) Fraction of differentially expressed genes in (**D**) bound by Nkx2-5 compared to the fraction expected by chance (red dotted line). Bars show 95% confidence intervals. Odds ratio and *P* value were obtained using Fisher's exact test. (**G**) Nkx2-5 ChIP-seq peaks proximal to differentially expressed genes in human hearts. (**H**) Percentage of differentially expressed genes that are bound by Nkx2-5.

 © 2020 The Authors. Published by Elsevier GmbH. This is an open access article under the CC BY-NC-ND license (http://creativecommons.org/licenses/by-nc-nd/4.0/).

genes that positively and 25 that negatively corelated with BMI (referred to as Mid-Cor) (Figure 6B). Similar to hearts at 8—9.4 weeks of gestation, positively corelated genes were enriched for functions related to lipid metabolism and mitochondrial function, while negatively correlated genes enriched for regulators of cell-ECM interactions and synapse regulatory pathways (Figure S13B). Despite the overlap in dysregulated pathways in hearts at early and mid-gestation, only six genes were commonly dysregulated. These results suggest that in association with a higher maternal BMI, pathways controlling mitochondrial oxidative metabolism were persistently overactivated and pathways regulating cell adhesion were repressed in the heart from early to mid-gestation.

3.8. Genes responsive to obesity *in utero* in the human fetal heart are developmentally regulated and enriched for Nkx2-5 targets

The expression of 91% of positively and 81% of negatively correlated Early-Cor genes maintained the same trend in hearts at 15.3 and 16.6 weeks of gestation (Figure S13C). Similarly, 98% of positively and 84% of negatively correlated Late-Cor genes maintained the same trend in hearts at 8—9.4 weeks of gestation (Figure S13D). However, the expression level of only 6 genes (*MT—ND3*, *MZT2B*, *MICOS13*, *SLC8A1-AS1*, *ANKRD36C*, and *SYCE1L*) significantly correlated with BMI in hearts at both early and mid-gestation. This suggested that different gene sets regulating common pathways respond differently to exposure to obesity *in utero* depending on the developmental stage. Indeed, the expression of Early-Cor and Mid-Cor genes is developmentally regulated. The expression level of genes that positively correlated with BMI was low at early and increased at mid-gestation. In contrast, the expression of negatively correlated genes was higher at early gestation but continuously decreased as gestation progressed (Figure 6C). This suggests that metabolism regulators expressed in the heart at mid-gestation are activated and cardiac development regulators expressed at early gestation are repressed in association with increased maternal BMI.

Gene expression was most drastically dysregulated in mouse CPs of embryos of the dams with the highest weight gain (Figure 5B). To determine whether morbid obesity is associated with gene dysregulation in the human fetal heart, we compared the hearts of 2 fetuses of morbidly obese (BMI 44.9 and 49.6) donors against age-matched (8—9.4 weeks) healthy (BMI 20.7—22.6) donors. After accounting for age and sex, 600 genes were dysregulated in hearts of fetuses of the morbidly obese donors (Figure 6D). GSEA revealed regulators of mitochondrial fatty acid oxidation as highly upregulated. Genes associated with ribosomal biogenesis and ECM remodeling such as ribosomal protein S24 (*RPS24*) and elastin (*ELN*), respectively, were also significantly upregulated (Figure 6E). These genes were also upregulated in 8-month-old mouse hearts born to the obese dams. Genes enriched for functions related to cardiac development were downregulated (Figure 6B). Notably, genes whose expression levels correlated with maternal BMI as a continuous variable were enriched for related functional categories (Figure S13A and B). Thus, human hearts of fetuses of the morbidly obese donors at 8—9.4 weeks of gestation overactivated gene networks regulating mitochondrial metabolism and translation and concomitantly downregulated networks controlling cell adhesion and heart development.

To determine whether Nkx2-5 targets genes dysregulated in the human fetal heart in response to obesity *in utero*, we cross-referenced dysregulated genes against published Nkx2-5 ChIP-seq datasets of differentiated human CMs [53]. Genes that were downregulated in the fetal hearts of morbidly obese donors enriched for direct Nkx2-5 targets (Figure 6F,G). Downregulated Nkx2-5 targets included *FLNC* involved in cell-ECM interactions [65] and cardiomyopathy-associated 1 (*XIRP1*) [66,67], both of which were also downregulated in adult mouse hearts born to the obese dams. Although upregulated genes were depleted of Nkx2-5 targets compared to genes that were not differentially expressed, ~20% were still bound by Nkx2-5 (Figure 6H). This was consistent with a higher enrichment of Nkx2-5 direct targets in genes downregulated in the heart of adult mice born to the obese dams (Figure 5L). This suggests that Nkx2-5 preferentially targets genes that are repressed in the mouse and human fetal heart in response to exposure to obesity *in utero*. Thus, disruption of Nkx2-5-controlled transcription sits high in the hierarchy of events embryonically programming heart disease susceptibility in response to maternal obesity.

4. DISCUSSION

The risk of adult-onset cardiovascular disease can be programmed in a fetus developing in an adverse environment [68]. Growing evidence from clinical studies points to maternal obesity as an important contributor to cardiovascular disease in progeny [2—4,6,7]. Accordingly, in mouse models of maternal obesity leading to diabetes and hyperglycemia, all the male offspring developed cardiac hypertrophy during adulthood [8—10,13]. However, hyperglycemia during human pregnancy leads to transient neonatal hypertrophy in offspring due to fetal hyperinsulinemia [69]. In addition, glucose levels in pregnant diabetic women are carefully monitored and controlled as part of standard medical care, suggesting that hyperglycemia is less likely to contribute to programming heart disease risk in humans. Indeed, obesity in the absence of diabetes during pregnancy negatively impacts the human fetal heart [6,7]. Although the offspring of obese women have a higher risk of cardiovascular disease, it is predominantly in older age and most of these individuals do not develop the disease [2—4], which suggests an increased susceptibility to disease rather than a predetermined disease trajectory.

Our study used a relatively mild obesogenic diet that caused a smaller gain in weight and body fat than previous models [70] that used more aggressive diets. Moreover, the diet used in our study did not alter glucose tolerance, which likely excluded the effects of chronic maternal hyperglycemia. In our model, male offspring developed a mild and progressive heart dysfunction in adulthood consistent with susceptibility to heart disease, more closely modeling the effects of maternal obesity in the progeny in humans. Our mice presented with normal glucose tolerance at conception. However, potential small increases in glucose levels representing a prediabetic state during pregnancy could not be excluded and factors including genetic background and housing conditions could have contributed to the different findings between studies.

We found that adults born to obese mice had normal heart function at 8 weeks of age (Table S3). However, heart function declined with aging and the hearts were overly responsive to pathologic stress. This supports a double-hit model in which obesity during pregnancy sensitizes offspring and secondary stress is required to elicit pathological responses in postnatal life. Accordingly, offspring born to the obese dams developed a reduced fractional shortening along with increased deposition of lipid droplets and ROS generation only when their metabolism was challenged with a high-fat diet [71]. This double-hit hypothesis is consistent with a higher risk of cardiovascular disease

 © 2020 The Authors. Published by Elsevier GmbH. This is an open access article under the CC BY-NC-ND license (http://creativecommons.org/licenses/by-nc-nd/4.0/).

in the progeny of obese women [2—4] and could explain why some individuals develop disease and others do not. This also suggests that different kinds of stress might elicit specific responses in hearts sensitized by maternal obesity. Linking phenotypes to specific molecular signatures in obese mothers and their offspring would facilitate predicting such responses and identifying individuals at a higher risk of cardiovascular disease.

Maternal weight was strongly correlated with the extent of gene dysregulation in the adult heart in the OH. Moreover, we found that IVRT positively correlated with maternal weight, indicating a direct correlation between maternal weight and the extent of diastolic dysfunction in the offspring. This is consistent with an increased risk of cardiovascular disease associated with higher BMIs in humans [2—4]. A key question is whether a threshold body weight or BMI beyond which genes and pathways affecting heart function are dysregulated in the offspring can be defined. Larger studies analyzing broader maternal weight and BMI distributions will be necessary to address this issue. Analyzing function and gene expression in hearts of fetuses of women with different BMIs during pregnancy and across different developmental stages would also be necessary. This requirement is highlighted by the small number of genes that were affected in CPs from embryos of dams spanning a narrow weight range when considering a maternal HD as a categorical variable (Figure 5A). Analyzing a higher number of embryos of dams spanning a broader weight range is required to determine the effect of diet and maternal weight. This illustrates that heterogeneity within groups can limit comparisons even when using mouse models and suggests that considering phenotype as a continuous variable would facilitate searching for predictors of disease risk programmed by maternal obesity.

Our transcriptomic analysis revealed that genes regulating ECM remodeling together with PI3K-AKT, TGF-β, and metabolic pathways were dysregulated in differentiating CPs and adult hearts in response to maternal obesity. We found that offspring of obese dams also had reduced diastolic function. Increased ECM deposition is known to increase cardiac stiffness, which can compromise ventricular compliance and reduce diastolic function [63,64]. We also found that genes in the PI3K-AKT and PPARα pathways were up- and downregulated, respectively (Figure 3C). Increased AKT activation leads to hypertrophy and ultimately heart failure and promotes increased glucose metabolism and reduced fatty acid oxidation by downregulation of PPARα [72]. The downregulation of the AKT targets AMPK and MTOR exclusively in adult hearts might be a compensatory attempt to maintain metabolic balance, but it could also lead to secondary activation of pro-inflammatory pathways [73], which was noted in 32-week-old OH (Figure 2B). Several ion channels, such as *Ryr2* and *Scn5a*, were exclusively downregulated in the 32-week-old adult hearts in the OH. Reduced expression of ion channels has been implicated in the development of arrhythmia during heart disease [74], consistent with our finding of bradycardia in the OH. Bradycardia was reported in a mouse model of maternal obesity and progressed to tachycardia with age [70]. This phenotype was hypothesized to be due to a defective response of baroreceptors in the heart [70]. However, our findings suggested that cardiac arrhythmia might be a primary phenotype resulting from abnormal ion channel expression. Thus, long-term dysregulation of specific pathways starting early in the developing heart and persistently in the adult heart explain heart disease predisposition in response to maternal obesity.

Comparing the genes differentially expressed in response to maternal obesity in CPs and adult hearts revealed numerous genes dysregulated exclusively in the adult hearts. However, some of these genes may have been dysregulated as a response to disease progression, and others might have become poised in CPs for dysregulation later in the adult hearts or in response to stress. This would require a mechanism for maintaining specific chromatin configurations in target genes over the long term. We found that genes regulating nucleosome assembly and DNA methylation were downregulated in CPs (Figure 5B). These processes stabilize gene expression and might have been involved in poising genes for dysregulation in the adult heart in our model. Gene repression mediated by trimethylation of lysine 27 and global DNA methylation are reduced in the heart in offspring born to obese dams [75] and could also contribute to long-term gene dysregulation in the heart. Long-term dysregulation of key transcription factors can program adult-onset heart disease [24]. Analysis of upstream and downstream regions of genes dysregulated in CPs and adult hearts in response to maternal obesity revealed enrichment of several transcription factor-binding motifs including Nkx2-5, ARID3A, and SRY, suggesting multiple potential mediators. However, our findings suggested a central function of Nkx2-5. *Nkx2-5* expression was reduced in CPs proportionally to maternal weight. In addition, Nkx2-5 targets were dysregulated in human fetal hearts of morbidly obese donors. *Nkx2-5* was not downregulated in adult hearts born to obese dams; however, Nkx2-5 direct targets were predominantly dysregulated. This suggested that transient downregulation of *Nkx2-5* in the embryonic heart could potentially lead to long-term dysregulation of its targets. Reducing the levels of Nkx2-5 alters the genome-wide binding of heterotypic complexes composed of Nkx2-5 and its regulatory partners. This leads to dysregulated transcription that disrupts heart development and can cause postnatal heart disease [16,52]. Future studies on the composition of Nkx2-5-containing complexes and their targets in hearts developing in the presence of maternal obesity will help address this possibility. Nkx2-5's dual role as an activator or repressor of gene expression could explain our finding that Nkx2-5 preferentially targets genes that are downregulated in CPs and upregulated in adult hearts in response to obesity during pregnancy. For example, Nkx2-5 represses the expression of target ion channels when interacting with Tbx3 but activates the same target genes when interacting with TBX5 [52]. Similarly, Nkx2-5 activates cardiac transcription networks but simultaneously represses gene expression via interactions with Hey2 in CPs [53]. In adult hearts in the OH, we found decreased expression of genes known to be activated by Nkx2-5 (Figure 4K) such as *Scn5a* [53]. In contrast, in CPs in embryos of the dams fed a HD, genes repressed by Nkx2-5 such as genes in the TGF-β signaling pathway [76] were upregulated (Figure 5K). Genes in the TGF-β pathway were also upregulated in adult hearts in the OH. Overactivating the TGF-β pathway promotes pathologic remodeling with increased fibrosis and inflammation in infarcted and pressure-overloaded hearts [77,78]. Thus, dysregulation of *Nkx2-5* and its target pathways sits high in the hierarchy of events programming an increased risk of heart disease in response to maternal obesity. Abnormal expression of *Nkx2-5* and its target pathways defines a state of heart disease susceptibility and a transcriptional signature that could be useful for early identification of individuals at a higher risk of heart disease.

AUTHOR CONTRIBUTIONS

Abdalla Ahmed: Methodology, investigation, formal analysis, visualization, and drafting original manuscript. **Minggao Liang:** Methodology and formal analysis. **Lijun Chi:** Methodology, investigation, and formal analysis. **Yu-Qing Zhou:** Methodology, investigation, and formal analysis. **John G. Sled:** Methodology, visualization, review, and editing. **Michael D. Wilson:** Methodology, investigation, formal

 © 2020 The Authors. Published by Elsevier GmbH. This is an open access article under the CC BY-NC-ND license (http://creativecommons.org/licenses/by-nc-nd/4.0/).

analysis, visualization, review, and editing. **Paul Delgado-Olguín:** Conceptualization, supervision, project administration, methodology, formal analysis, funding, review and editing.

FUNDING

This study was supported by the Canadian Institutes of Health Research (CIHR) (162208 and 149046), the Heart and Stroke Foundation of Canada (G-17-0018613), the Natural Sciences and Engineering Research Council of Canada (NSERC) (500865), Operational Funds from the Hospital for Sick Children (P.D.O.), and the Ted Rogers Center for Heart Research (A.A.). M.W. was supported by the Canada Research Chairs Program and an Early Researcher Award from the Ontario Ministry of Research and Innovation.

ACKNOWLEDGMENTS

We thank Sergio Pereira (the Center for Applied Genomics) for sequencing, Laura Caporiccio for mouse colony management, Sina Fatehi and Etri Kocaqi for help with the experiments, the Center for Phenogenomics for mouse husbandry, the Daniel Drucker lab for access and guidance with the EchoMRI-100 machine, the Lee Adamson lab for access to and guidance with the echocardiography equipment, the Mount Sinai Biobank for facilitating access to human heart specimens, and the Sick Kids-UHN Flow Cytometry Core Facility for help with cell sorting. We also thank Koroboshka Brand-Arzamendi for artwork in the graphical abstract.

CONFLICT OF INTEREST

None declared.

APPENDIX A. SUPPLEMENTARY DATA

Supplementary data to this article can be found online at https://doi.org/10.1016/j.molmet.2020.101116.

REFERENCES

[1] Ahmed, A., Delgado-Olguin, P., 2020. Embryonic programming of heart disease in response to obesity during pregnancy. Biochimica et Biophysica Acta - Molecular Basis of Disease 1866(2):165402. https://doi.org/10.1016/j.bbadis.2019.01.028.

[2] Reynolds, R.M., Allan, K.M., Raja, E.a., Bhattacharya, S., McNeill, G., Hannaford, P.C., et al., 2013. Maternal obesity during pregnancy and premature mortality from cardiovascular event in adult offspring: follow-up of 1 323 275 person years. BMJ 347(August):f4539. https://doi.org/10.1136/bmj.f4539.

[3] Forsén, T., Eriksson, J.G., Tuomilehto, J., Teramo, K., Osmond, C., Barker, D.J., 1997. Mother's weight in pregnancy and coronary heart disease in a cohort of Finnish men: follow up study. BMJ (Clinical Research Ed.) 315(7112):837–840. https://doi.org/10.1136/bmj.315.7112.837.

[4] Eriksson, J.G., Sandboge, S., Salonen, M.K., Kajantie, E., Osmond, C., 2014. Long-term consequences of maternal overweight in pregnancy on offspring later health: findings from the Helsinki Birth Cohort Study. Annals of Medicine 3890(April):1–5. https://doi.org/10.3109/07853890.2014.919728.

[5] Asrani, P., Pinto, N., Puchalski, M., Ou, Z., Silver, R.M., Zinkhan, E.K., et al., 2020. Maternal predictors of disparate outcomes in children with single ventricle congenital heart disease. Journal of the American Heart Association 9(12):e014363.

[6] Ece, I., Uner, A., Balli, S., Kibar, A.E., Oflaz, M.B., Kurdoglu, M., 2014. The effects of pre-pregnancy obesity on fetal cardiac functions. Pediatric Cardiology 35(5):838–843. https://doi.org/10.1007/s00246-014-0863-0.

[7] Ingul, C.B., Lorås, L., Tegnander, E., Eik-Nes, S.H., Brantberg, A., 2016. Maternal obesity affects fetal myocardial function as early as in the first trimester. Ultrasound in Obstetrics and Gynecology 47(4):433–442. https://doi.org/10.1002/uog.14841.

[8] Fernandez-Twinn, D.S., Blackmore, H.L., Siggens, L., Giussani, D.A., Cross, C.M., Foo, R., et al., 2012. The programming of cardiac hypertrophy in the offspring by maternal obesity is associated with hyperinsulinemia, AKT, ERK, and mTOR activation. Endocrinology 153(12):5961–5971. https://doi.org/10.1210/en.2012-1508.

[9] Beeson, J.H., Blackmore, H.L., Carr, S.K., Dearden, L., Duque-Guimarães, D.E., Kusinski, L.C., et al., 2018. Maternal exercise intervention in obese pregnancy improves the cardiovascular health of the adult male offspring. Molecular Metabolism 16:35–44. https://doi.org/10.1016/j.molmet.2018.06.009.

[10] Loche, E., Blackmore, H.L., Carpenter, A.A., Beeson, J.H., Pinnock, A., Ashmore, T.J., et al., 2018. Maternal diet-induced obesity programmes cardiac dysfunction in male mice independently of post-weaning diet. Cardiovascular Research 114(10):1372–1384. https://doi.org/10.1093/cvr/cvy082.

[11] Ghnenis, A.B., Odhiambo, J.F., McCormick, R.J., Nathanielsz, P.W., Ford, S.P., 2017. Maternal obesity in the Ewe increases cardiac ventricular expression of glucocorticoid receptors, proinflammatory cytokines and fibrosis in adult male offspring. PLoS ONE. https://doi.org/10.1371/journal.pone.0189977.

[12] Guida, M.C., Birse, R.T., Dall'Agnese, A., Toto, P.C., Diop, S.B., Mai, A., et al., 2019. Intergenerational inheritance of high fat diet-induced cardiac lipotoxicity in Drosophila. Nature Communications. https://doi.org/10.1038/s41467-018-08128-3.

[13] Blackmore, H.L., Niu, Y., Fernandez-Twinn, D.S., Tarry-Adkins, J.L., Giussani, D.A., Ozanne, S.E., 2014. Maternal diet-induced obesity programs cardiovascular dysfunction in adult male mouse offspring independent of current body weight. Endocrinology 155(10):3970–3980. https://doi.org/10.1210/en.2014-1383.

[14] Wang, G., Huang, W.Q., Cui, S.D., Li, S., Wang, X.Y., Li, Y., et al., 2015. Autophagy is involved in high glucose-induced heart tube malformation. Cell Cycle 14(5):772–783. https://doi.org/10.1080/15384101.2014.1000170.

[15] Hachisuga, M., Oki, S., Kitajima, K., Ikuta, S., Sumi, T., Kato, K., et al., 2015. Hyperglycemia impairs left-right axis formation and thereby disturbs heart morphogenesis in mouse embryos. Proceedings of the National Academy of Sciences of the United States of America 112(38):E5300–E5307. https://doi.org/10.1073/pnas.1504529112.

[16] Luna-Zurita, L., Stirnimann, C.U., Glatt, S., Kaynak, B.L., Thomas, S., Baudin, F., et al., 2016. Complex interdependence regulates heterotypic transcription factor distribution and coordinates cardiogenesis. Cell 164(5):999–1014. https://doi.org/10.1016/j.cell.2016.01.004.

[17] Kasahara, H., Bartunkova, S., Schinke, M., Tanaka, M., Izumo, S., 1998. Cardiac and extracardiac expression of Csx/Nkx2.5 homeodomain protein. Circulation Research 82(9):934–936. https://doi.org/10.1161/01.RES.82.9.936.

[18] Hu, B., Wu, Y.M., Wu, Z., Phan, S.H., 2010. Nkx2.5/Csx represses myofibroblast differentiation. American Journal of Respiratory Cell and Molecular Biology 42(2):218–226. https://doi.org/10.1165/rcmb.2008-0404OC.

[19] Kim, H.S., Woo, J.S., Joo, H.J., Moon, W.K., 2012. Cardiac transcription factor Nkx2.5 is downregulated under excessive O-GlcNAcylation condition. PLoS ONE 7(6):e38053. https://doi.org/10.1371/journal.pone.0038053.

[20] Furtado, M.B., Wilmanns, J.C., Chandran, A., Perera, J., Hon, O., Biben, C., et al., 2017. Point mutations in murine Nkx2-5 phenocopy human congenital heart disease and induce pathogenic Wnt signaling. JCI Insight 2(6):e88271. https://doi.org/10.1172/jci.insight.88271.

[21] Sun, Y., Wang, Q., Fang, Y., Wu, C., Lu, G., Chen, Z., 2017. Activation of the Nkx2.5-Calr-p53 signaling pathway by hyperglycemia induces cardiac remodeling and dysfunction in adult zebrafish. DMM Disease Models and Mechanisms 10(10):1217–1227. https://doi.org/10.1242/dmm.026781.

 © 2020 The Authors. Published by Elsevier GmbH. This is an open access article under the CC BY-NC-ND license (http://creativecommons.org/licenses/by-nc-nd/4.0/).

[22] Briggs, L.E., Takeda, M., Cuadra, A.E., Wakimoto, H., Marks, M.H., Walker, A.J., et al., 2008. Perinatal loss of Nkx2-5 results in rapid conduction and contraction defects. Circulation Research 103(6):580–590. https://doi.org/10.1161/CIRCRESAHA.108.171835.

[23] Toko, H., Zhu, W., Takimoto, E., Shiojima, I., Hiroi, Y., Zou, Y., et al., 2002. Csx/Nkx2-5 is required for homeostasis and survival of cardiac myocytes in the adult heart. Journal of Biological Chemistry 277(27):24735–24743. https://doi.org/10.1074/jbc.M107669200.

[24] Delgado-Olguín, P., Huang, Y., Li, X., Christodoulou, D., Seidman, C.E., Seidman, J.G., et al., 2012. Epigenetic repression of cardiac progenitor gene expression by Ezh2 is required for postnatal cardiac homeostasis. Nature Genetics 44(3):343–347. https://doi.org/10.1038/ng.1068.

[25] Hsiao, E.C., Yoshinaga, Y., Nguyen, T.D., Musone, S.L., Kim, J.E., Swinton, P., et al., 2008. Marking embryonic stem cells with a 2A self-cleaving peptide: a NKX2-5 emerald GFP BAC reporter. PloS One 3(7):e2532. https://doi.org/10.1371/journal.pone.0002532.

[26] Zhou, Y.Q., Zhu, Y., Bishop, J., Davidson, L., Henkelman, R.M., Bruneau, B.G., et al., 2005. Abnormal cardiac inflow patterns during postnatal development in a mouse model of Holt-Oram syndrome. American Journal of Physiology - Heart and Circulatory Physiology 289(3):H992–H1001. https://doi.org/10.1152/ajpheart.00027.2005.

[27] Li, P., Sur, S.H., Mistlberger, R.E., Morris, M., 1999. Circadian blood pressure and heart rate rhythms in mice. American Journal of Physiology - Regulatory, Integrative and Comparative Physiology 276(2):R500–R504. https://doi.org/10.1152/ajpregu.1999.276.2.r500.

[28] Roy, A.R., Ahmed, A., DiStefano, P.V., Chi, L., Khyzha, N., Galjart, N., et al., 2018. The transcriptional regulator CCCTC-binding factor limits oxidative stress in endothelial cells. Journal of Biological Chemistry 293(22):8449–8461. https://doi.org/10.1074/jbc.M117.814699.

[29] Ahmed, A., Delgado-Olguin, P., 2018. Isolating embryonic cardiac progenitors and cardiac myocytes by fluorescence-activated cell sorting, vol. 1752.

[30] Bolger, A.M., Lohse, M., Usadel, B., 2014. Trimmomatic: a flexible trimmer for Illumina sequence data. Bioinformatics 30(15):2114–2120. https://doi.org/10.1093/bioinformatics/btu170.

[31] Dobin, A., Davis, C.A., Schlesinger, F., Drenkow, J., Zaleski, C., Jha, S., et al., 2013. STAR: ultrafast universal RNA-seq aligner. Bioinformatics 29(1):15–21. https://doi.org/10.1093/bioinformatics/bts635.

[32] Liao, Y., Smyth, G.K., Shi, W., 2014. FeatureCounts: an efficient general purpose program for assigning sequence reads to genomic features. Bioinformatics 30(7):923–930. https://doi.org/10.1093/bioinformatics/btt656.

[33] Love, M.I., Huber, W., Anders, S., 2014. Moderated estimation of fold change and dispersion for RNA-seq data with DESeq2. Genome Biology 15(12):550. https://doi.org/10.1186/s13059-014-0550-8.

[34] Plotly Technologies Inc., 2015. Plotly for R. Collaborative data science publisher. Plotly Technologies Inc.. https://plot.ly.

[35] de Hoon, M.J.L., Imoto, S., Nolan, J., Miyano, S., 2004. Open source clustering software. Bioinformatics 20(9):1453–1454. https://doi.org/10.1093/bioinformatics/bth078.

[36] Huang, D.W., Sherman, B.T., Lempicki, R.A., 2009. Bioinformatics enrichment tools: paths toward the comprehensive functional analysis of large gene lists. Nucleic Acids Research 37(1):1–13. https://doi.org/10.1093/nar/gkn923.

[37] Huang, D.W., Sherman, B.T., Lempicki, R.A., 2009. Systematic and integrative analysis of large gene lists using DAVID bioinformatics resources. Nature Protocols 4(1):44–57. https://doi.org/10.1038/nprot.2008.211.

[38] Kwon, A.T., Arenillas, D.J., Hunt, R.W., Wasserman, W.W., 2012. Opossum-3: advanced analysis of regulatory motif over-representation across genes or chip-seq datasets. G3: Genes, Genomes, Genetics 2(9):987–1002. https://doi.org/10.1534/g3.112.003202.

[39] Mootha, V.K., Lindgren, C.M., Eriksson, K.F., Subramanian, A., Sihag, S., Lehar, J., et al., 2003. PGC-1α-responsive genes involved in oxidative phosphorylation are coordinately downregulated in human diabetes. Nature Genetics 34(3):267–273. https://doi.org/10.1038/ng1180.

[40] Subramanian, A., Tamayo, P., Mootha, V.K., Mukherjee, S., Ebert, B.L., Gillette, M.A., et al., 2005. Gene set enrichment analysis: a knowledge-based approach for interpreting genome-wide expression profiles. Proceedings of the National Academy of Sciences of the United States of America 102(43):15545–15550. https://doi.org/10.1073/pnas.0506580102.

[41] Shannon, P., Markiel, A., Ozier, O., Baliga, N.S., Wang, J.T., Ramage, D., et al., 2003. Cytoscape: a software Environment for integrated models of biomolecular interaction networks. Genome Research 13(11):2498–2504. https://doi.org/10.1101/gr.1239303.

[42] Merico, D., Isserlin, R., Stueker, O., Emili, A., Bader, G.D., 2010. Enrichment map: a network-based method for gene-set enrichment visualization and interpretation. PloS One 5(11):e13984. https://doi.org/10.1371/journal.pone.0013984.

[43] Kucera, M., Isserlin, R., Arkhangorodsky, A., Bader, G.D., 2016. AutoAnnotate: a Cytoscape app for summarizing networks with semantic annotations. F1000Research 5:1717. https://doi.org/10.12688/F1000RESEARCH.9090.1.

[44] Reimand, J., Isserlin, R., Voisin, V., Kucera, M., Tannus-Lopes, C., Rostamianfar, A., et al., 2019. Pathway enrichment analysis and visualization of omics data using g:Profiler, GSEA, Cytoscape and EnrichmentMap. Nature Protocols 14(2):482–517. https://doi.org/10.1038/s41596-018-0103-9.

[45] Prunotto, A., Stevenson, B.J., Berthonneche, C., Schüpfer, F., Beckmann, J.S., Maurer, F., et al., 2016. RNAseq analysis of heart tissue from mice treated with atenolol and isoproterenol reveals a reciprocal transcriptional response. BMC Genomics 17(1):717. https://doi.org/10.1186/s12864-016-3059-6.

[46] Ma, X., Gao, L., Karamanlidis, G., Gao, P., Lee, C.F., Garcia-Menendez, L., et al., 2015. Revealing pathway dynamics in heart diseases by analyzing multiple differential networks. PLoS Computational Biology 11(6):e1004332. https://doi.org/10.1371/journal.pcbi.1004332.

[47] Song, H.K., Hong, S.E., Kim, T., Kim, D.H., 2012. Deep RNA sequencing reveals novel cardiac transcriptomic signatures for physiological and pathological hypertrophy. PloS One 7(4):e35552. https://doi.org/10.1371/journal.pone.0035552.

[48] Kesherwani, V., Shahshahan, H.R., Mishra, P.K., 2017. Cardiac transcriptome profiling of diabetic Akita mice using microarray and next generation sequencing. PloS One 12(8):e0182828. https://doi.org/10.1371/journal.pone.0182828.

[49] Liu, X., Ma, Y., Yin, K., Li, W., Chen, W., Zhang, Y., et al., 2019. Long non-coding and coding RNA profiling using strand-specific RNA-seq in human hypertrophic cardiomyopathy. Scientific Data 6(1):90. https://doi.org/10.1038/s41597-019-0094-6.

[50] Sweet, M.E., Cocciolo, A., Slavov, D., Jones, K.L., Sweet, J.R., Graw, S.L., et al., 2018. Transcriptome analysis of human heart failure reveals dysregulated cell adhesion in dilated cardiomyopathy and activated immune pathways in ischemic heart failure. BMC Genomics 19(1):812. https://doi.org/10.1186/s12864-018-5213-9.

[51] Warde-Farley, D., Donaldson, S.L., Comes, O., Zuberi, K., Badrawi, R., Chao, P., et al., 2010. The GeneMANIA prediction server: biological network integration for gene prioritization and predicting gene function. Nucleic Acids Research 38(Web Server issue):W214–W220. https://doi.org/10.1093/nar/gkq537.

[52] Van Den Boogaard, M., Wong, L.Y.E., Tessadori, F., Bakker, M.L., Dreizehnter, L.K., Wakker, V., et al., 2012. Genetic variation in T-box binding element functionally affects SCN5A/SCN10A enhancer. Journal of Clinical Investigation 122(7):2519–2530. https://doi.org/10.1172/JCI62613.

[53] Anderson, D.J., Kaplan, D.I., Bell, K.M., Koutsis, K., Haynes, J.M., Mills, R.J., et al., 2018. NKX2-5 regulates human cardiomyogenesis via a HEY2 dependent transcriptional network. Nature Communications 9(1):1373. https://doi.org/10.1038/s41467-018-03714-x.

 © 2020 The Authors. Published by Elsevier GmbH. This is an open access article under the CC BY-NC-ND license (http://creativecommons.org/licenses/by-nc-nd/4.0/).

[54] McLean, C.Y., Bristor, D., Hiller, M., Clarke, S.L., Schaar, B.T., Lowe, C.B., et al., 2010. GREAT improves functional interpretation of cis-regulatory regions. Nature Biotechnology 28(5):495—501. https://doi.org/10.1038/nbt.1630.

[55] Mottram, P.M., Marwick, T.H., 2005. Assessment of diastolic function: what the general cardiologist needs to know. Heart 91(5):681—695. https://doi.org/10.1136/hrt.2003.029413 (5).

[56] Kuzuya, M., Enoki, H., Iwata, M., Hasegawa, J., Hirakawa, Y., 2008. J-shaped relationship between resting pulse rate and all-cause mortality in community-dwelling older people with disabilities. Journal of the American Geriatrics Society 56(2):367—368. https://doi.org/10.1111/j.1532-5415.2007.01512.x.

[57] Dirkx, E., da Costa Martins, P.A., De Windt, L.J., 2013. Regulation of fetal gene expression in heart failure. Biochimica et Biophysica Acta - Molecular Basis of Disease 1832(12):2414—2424. https://doi.org/10.1016/j.bbadis.2013.07.023.

[58] Suwanabol, P.A., Seedial, S.M., Zhang, F., Shi, X., Si, Y., Liu, B., et al., 2012. TGF-β and Smad3 modulate PI3K/Akt signaling pathway in vascular smooth muscle cells. American Journal of Physiology - Heart and Circulatory Physiology 302(11):H2211—H2219. https://doi.org/10.1152/ajpheart.00966.2011.

[59] Jia, G., Hill, M.A., Sowers, J.R., 2018. Diabetic cardiomyopathy: an update of mechanisms contributing to this clinical entity. Circulation Research 122(4):624—638. https://doi.org/10.1161/CIRCRESAHA.117.311586.

[60] Wang, J.J.C., Rau, C., Avetisyan, R., Ren, S., Romay, M.C., Stolin, G., et al., 2016. Genetic dissection of cardiac remodeling in an isoproterenol-induced heart failure mouse model. PLoS Genetics 12(7):e1006038. https://doi.org/10.1371/journal.pgen.1006038.

[61] Kuusisto, J., Kärjä, V., Sipola, P., Kholová, I., Peuhkurinen, K., Jääskeläinen, P., et al., 2012. Low-grade inflammation and the phenotypic expression of myocardial fibrosis in hypertrophic cardiomyopathy. Heart 98(13):1007—1013. https://doi.org/10.1136/heartjnl-2011-300960.

[62] Smeets, P.J.H., Teunissen, B.E.J., Willemsen, P.H.M., Van Nieuwenhoven, F.A., Brouns, A.E., Janssen, B.J.A., et al., 2008. Cardiac hypertrophy is enhanced in PPARα-/- mice in response to chronic pressure overload. Cardiovascular Research 78(1):79—89. https://doi.org/10.1093/cvr/cvn001.

[63] Røe, Å.T., Aronsen, J.M., Skårdal, K., Hamdani, N., Linke, W.A., Danielsen, H.E., et al., 2017. Increased passive stiffness promotes diastolic dysfunction despite improved Ca2+ handling during left ventricular concentric hypertrophy. Cardiovascular Research 113(10):1161—1172. https://doi.org/10.1093/cvr/cvx087.

[64] Burlew, B.S., Weber, K.T., 2002. Cardiac fibrosis as a cause of diastolic dysfunction. Herz 27(2):92—98. https://doi.org/10.1007/s00059-002-2354-y.

[65] Nakamura, F., Stossel, T.P., Hartwig, J.H., 2011. The filamins: organizers of cell structure and function. Cell Adhesion & Migration. https://doi.org/10.4161/cam.5.2.14401.

[66] Otten, J., Van Der Ven, P.F.M., Vakeel, P., Eulitz, S., Kirfel, G., Brandau, O., et al., 2010. Complete loss of murine Xin results in a mild cardiac phenotype with altered distribution of intercalated discs. Cardiovascular Research. https://doi.org/10.1093/cvr/cvp345.

[67] Huang, L., Wu, K.H., Zhang, L., Wang, Q., Tang, S., Wu, Q., et al., 2018. Critical roles of Xirp proteins in cardiac conduction and their rare variants identified in sudden unexplained nocturnal death syndrome and Brugada syndrome in Chinese han population. Journal of the American Heart Association. https://doi.org/10.1161/JAHA.117.006320.

[68] Cohen, E., Wong, F.Y., Horne, R.S.C., Yiallourou, S.R., 2016. Intrauterine growth restriction: impact on cardiovascular development and function throughout infancy. Pediatric Research 79(6):821—830. https://doi.org/10.1038/pr.2016.24.

[69] Paauw, N.D., Stegeman, R., de Vroede, M.A.M.J., Termote, J.U.M., Freund, M.W., Breur, J.M.P.J., 2020. Neonatal cardiac hypertrophy: the role of hyperinsulinism—a review of literature. European Journal of Pediatrics 179(1):39—50. https://doi.org/10.1007/s00431-019-03521-6.

[70] Samuelsson, A.M., Matthews, P.A., Argenton, M., Christie, M.R., McConnell, J.M., Jansen, E.H.J.M., et al., 2008. Diet-induced obesity in female mice leads to offspring hyperphagia, adiposity, hypertension, and insulin resistance: a novel murine model of developmental programming. Hypertension 51(2):383—392. https://doi.org/10.1161/HYPERTENSIONAHA.107.101477.

[71] Turdi, S., Ge, W., Hu, N., Bradley, K.M., Wang, X., Ren, J., 2013. Interaction between maternal and postnatal high fat diet leads to a greater risk of myocardial dysfunction in offspring via enhanced lipotoxicity, IRS-1 serine phosphorylation and mitochondrial defects. Journal of Molecular and Cellular Cardiology 55:117—129. https://doi.org/10.1016/j.yjmcc.2012.12.007.

[72] Chaanine, A.H., Hajjar, R.J., 2011. AKT signalling in the failing heart. European Journal of Heart Failure 13(8):825—829. https://doi.org/10.1093/eurjhf/hfr080.

[73] Aoyagi, T., Matsui, T., 2011. Phosphoinositide-3 kinase signaling in cardiac hypertrophy and heart failure. Current Pharmaceutical Design 17(18):1818—1824. https://doi.org/10.2174/138161211796390976.

[74] Nattel, S., Maguy, A., Le Bouter, S., Yeh, Y.H., 2007. Arrhythmogenic ion-channel remodeling in the heart: heart failure, myocardial infarction, and atrial fibrillation. Physiological Reviews 87(2):425—456. https://doi.org/10.1152/physrev.00014.2006.

[75] Blin, G., Liand, M., Mauduit, C., Chehade, H., Benahmed, M., Simeoni, U., et al., 2020. Maternal exposure to high-fat diet induces long-term derepressive chromatin marks in the heart. Nutrients 12(1):181. https://doi.org/10.3390/nu12010181.

[76] Prall, O.W.J., Menon, M.K., Solloway, M.J., Watanabe, Y., Zaffran, S., Bajolle, F., et al., 2007. An Nkx2-5/Bmp2/smad1 negative feedback loop controls heart progenitor specification and proliferation. Cell 128(5):947—959. https://doi.org/10.1016/j.cell.2007.01.042.

[77] Xia, Y., Lee, K., Li, N., Corbett, D., Mendoza, L., Frangogiannis, N.G., 2009. Characterization of the inflammatory and fibrotic response in a mouse model of cardiac pressure overload. Histochemistry and Cell Biology 131(4):471—481. https://doi.org/10.1007/s00418-008-0541-5.

[78] Bujak, M., Ren, G., Kweon, H.J., Dobaczewski, M., Reddy, A., Taffet, G., et al., 2007. Essential role of Smad3 in infarct healing and in the pathogenesis of cardiac remodeling. Circulation 116(19):2127—2138. https://doi.org/10.1161/CIRCULATIONAHA.107.704197.

 © 2020 The Authors. Published by Elsevier GmbH. This is an open access article under the CC BY-NC-ND license (http://creativecommons.org/licenses/by-nc-nd/4.0/).